GEOLOGICA CARPATHICA, 52, 6, BRATISLAVA, DECEMBER 2001
327–342

GEOCHEMISTRY OF TRIASSIC RADIOLARIAN CHERTS IN NORTH-WESTERN CROATIA

JOSIP HALAMIĆ[1], VESNA MARCHIG[2] and ŠPELA GORIČAN[3]

[1]Institute of Geology, Sachsova 2, HR-10000 Zagreb, Croatia; jhalamic@yahoo.com
[2]Bundesanstalt für Geowissenschaften und Rohstoffe, Stilleweg 2, D-30631 Hannover, Germany; v.marchig@bgr.de
[3]Institute of Paleontology, ZRC SAZU, Gosposka 13, SI-1000 Ljubljana, Slovenia; spela@zrc-sazu.si

(Manuscript received April 18, 2001; accepted in revised form October 5, 2001)

Abstract: The analysed Triassic (Illyrian, Lower Fassanian, Upper Carnian) radiolarian cherts on Žumberak, Ivanščica, Kalnik and Medvednica Mts (NW Croatia) are rocks with high SiO_2 content (mean >90 %) and the major part of silica is of biogenic origin. Besides this siliceous component, two others stand out in the radiolarian cherts. One of them is detritic (terrigenous input) and it consists mainly of Al, Ti, K, Zr, Hf, Cr, Th, Rb, Nb and Sc. The other, hydrothermal one, is composed of Fe, Mn, P, Cu, Pb, Zn, Ni, Co and Sr. The terrigenous component is a significant REE carrier. The radiolarian cherts on Kalnik and Medvednica Mts show a positive Ce-anomaly (Ce/Ce*) which indicates a sedimentation in a narrow trough relatively close to the continent. The negative Ce-anomaly on Žumberak and Ivanščica Mts suggests a reduced terrigenous input. The radiolarian cherts in the last mentioned areas are sedimented directly onto the dolomites and limestones of the carbonate platform. This means that the terrigenous input was probably weaker, because of the width of the disintegrated carbonate platform (larger distance to the continent) or because of a topographically higher position (bypass of fine terrigenous material) with respect to Medvednica and Kalnik.

Key words: South-western Pannonian region, NW Dinarides, Croatia, Triassic, radiolarian cherts, geochemistry, major and trace elements, REE.

Introduction

The area of north-western Croatia is situated within the south-western part of the Pannonian region (Fig. 1). Because of its placement in relation to the Alps, Dinarides and Pannonian Basin it is essential for solving the tectonic and paleogeographic relationships of this part of the Tethys.

The radiolarites are especially interesting, forming the upper part of an ophiolitic sequence (geophysical layer 1 — Wilson 1989). In north-western Croatia they often occur in the Middle and Upper Triassic marine sediments. On Žumberak Mt and part of Ivanščica Mt (Fig. 1) these rocks are part of the Middle Triassic volcano-sedimentary formation and they occur together with pyroclastics and basic volcanites within the carbonate complex (Šikić et al. 1979; Basch 1983; Šimunić et al. 1981; Šimunić & Šimunić 1980, 1997; Bukovac et al. 1995; Grgasović et al. 2000). During the Late Jurassic and Early Cretaceous, the Middle to Upper Triassic siliceous rocks from Kalnik Mt, part of Ivanščica and Medvednica Mts were incorporated into an accretionary prism (subductional complex) and today they represent part of an ophiolitic melánge (Halamić & Goričan 1995; Halamić 1998; Pamić & Tomljenović 1998; Grgasović et al. 2000).

In the past the Triassic siliceous rocks were described only sporadically and their age was determined on the basis of their superpositional relation to the other sedimentary rocks defined by their fossil content. The exact stratigraphic position of the radiolarites has been documented in the recent publications (Halamić & Goričan 1995; Halamić 1998; Grgasović et al. 2000).

Up to now, the chemical composition (major and trace elements and REE) of these rocks was poorly known. In recent publications, Halamić & Goričan (1995) and Halamić (1998) tried to determine the original tectonic and depositional environment of the radiolarites from the Kalnik and Medvednica Mts on the basis of the chemical composition of major elements and their ratios.

In this paper we show detailed geochemical study (major, trace, and rare earth elements) of radiolarian cherts from radiolarite succession of selected localities in north-western Croatia and try to explain depositional environment of radiolarian oozes. Due to the tectonic position of the investigated area, we consider that this paper is an important contribution to better understanding of the geological evolution of this part of the Tethys during the Triassic which will enable comparison with similar siliceous rocks in the Alps, Dinarides, Hellenides, Pannonian region and Carpathians.

Geological setting, basic geological data and petrographical outline

The investigated area is situated in the SW part of the Pannonian region (Fig. 1). According to Haas et al. (1990, 1995, 2000), it represents the SW extension of the Mid-Transdanubian Terrain, that is the Zagorje-Mid-Transdanubian Zone (Pamić & Tomljenović 1998). This terrain is separated towards the SE from the Tisza Megaunit by the Zagreb-Zemplen lineament (Kovács et al. 1988) and towards NW from Transdanubian Central Range subunit by the Periadriatic lineament (Fig. 1). According to Herak (1986) this area represents a part of the Supradinaric geodynamic unit, or Inner Dinarides (Herak et al. 1990).

The major part of north-western Croatia is covered by Cenozoic sediments. Under this cover there are Mesozoic rocks

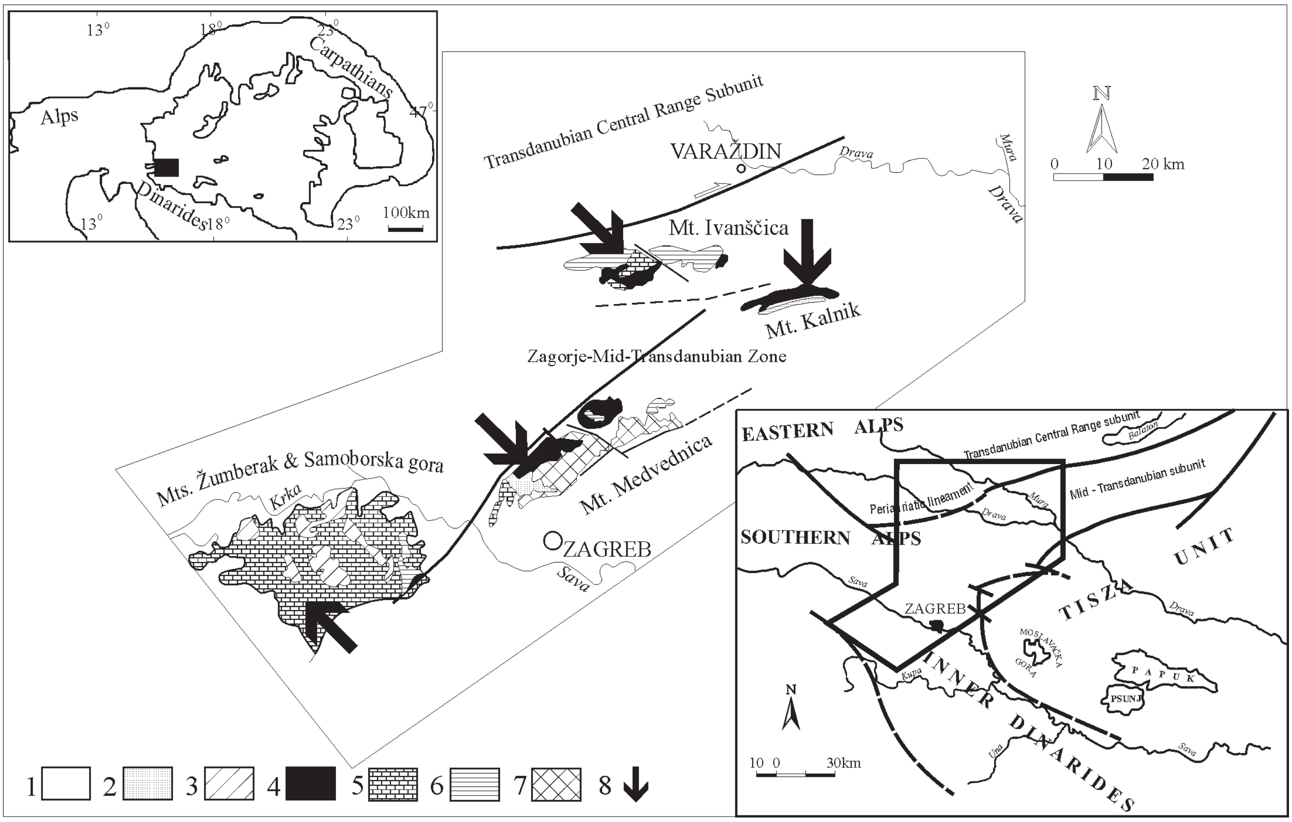

Fig. 1. Location map and geological sketch map of north-western Croatia (according to Pamić & Tomljenović 1998, supplemented) with locations of analysed sections. *Legend:* 1 — Neogene and Quaternary fill of the Pannonian Basin; 2 — Late Cretaceous-Paleocene flysch; 3 — Hauterivian to Cenomanian pelagic limestones and calcareous turbidites; 4 — Ophiolitic melánge; 5 — Late Triassic platform carbonates; 6 — Late Paleozoic and Triassic clastics and carbonates interlayered with volcanics and tuffs; 7 — Paleozoic-Triassic metamorphic complex; 8 — Section position.

forming the cores of the Žumberak, Kalnik, Medvednica, and Ivanščica Mts. The central part of the Medvednica Mt consists of Paleozoic-Mesozoic metamorphic rocks (Fig. 1).

During the preparation of the Geological Map of the Republic of Croatia (scale 1:50,000), the representative geological sections of Triassic deep-water sediments were investigated on Žumberak Mt (Kolići and Bezjak sections), Ivanščica Mt (Belski dol 1 and 2 sections), Kalnik Mt (Jazvina, VHK, Kestenik sections) and Medvednica Mt (PC and PF sections) (Bukovac et al. 1995; Halamić & Goričan 1995; Šimunić & Šimunić 1997; Halamić 1998; Grgasović et al. 2000). In these papers basic geological data on these rocks was presented and on the basis of paleontological results the age was determined.

For present investigation only radiolarian cherts from radiolarite succession (chert/shale couplets) were sampled at nine sections which were representative for the investigated area. Only samples which were determined as Triassic (42 in total) by previous research were selected for chemical analysis (Halamić & Goričan 1995; Halamić 1998; Grgasović et al. 2000).

The Kolići section (KL) (1 on Fig. 2). The red radiolarian cherts were found in the lower part of the section with intercalations of siltites and pyroclastites. The analysis of the radiolarian fauna shows its Late Anisian to Early Ladinian age.

The matrix of cherts is composed of microcrystalline quartz and recrystallized radiolarian tests. White micas and clay minerals form clastic detritus. Preserved radiolarian tests are filled up with microcrystalline quartz and radial chalcedony. Accessory minerals are rounded zircon, opaque mineral grains and apatite. There are preserved parts of microcrystalline calcite in the matrix (sample KL-70).

The Bezjak section (BZ) (2 on Fig. 2). The interval of siliceous rocks was found in the lower part of the section. It is composed of cm- to dm-beds of greenish-gray radiolarian cherts with interstratified tuffitic siltstones. The Late Anisian (Illyrian) age is determined on the basis of radiolarians.

Siliceous rocks are determined as dolomitized radiolarian cherts. The rock matrix is built of microcrystalline quartz with relics of microcrystalline calcite and dolomitization is visible in the form of small dolomite crystals. In the matrix, there are recrystallized and partly dolomitized radiolarian skeletons. The accessory minerals are apatite, hematite and rare rounded zircon.

The Belski dol-1 section (BD-II) (3 on Fig. 2). The silicified grayish pelecypod limestones, greenish pyroclastites and red radiolarian cherts in alternation overlie carbonate breccias with "pseudooncoidal" structure. Cherts are found in the lower part of the interval and their age is defined as Early Ladinian (Early Fassanian).

The rock matrix consists of microcrystalline quartz and is rich in ferruginous substance. Radiolarian skeletons are filled with granular quartz. In the matrix, there are also submillimet-

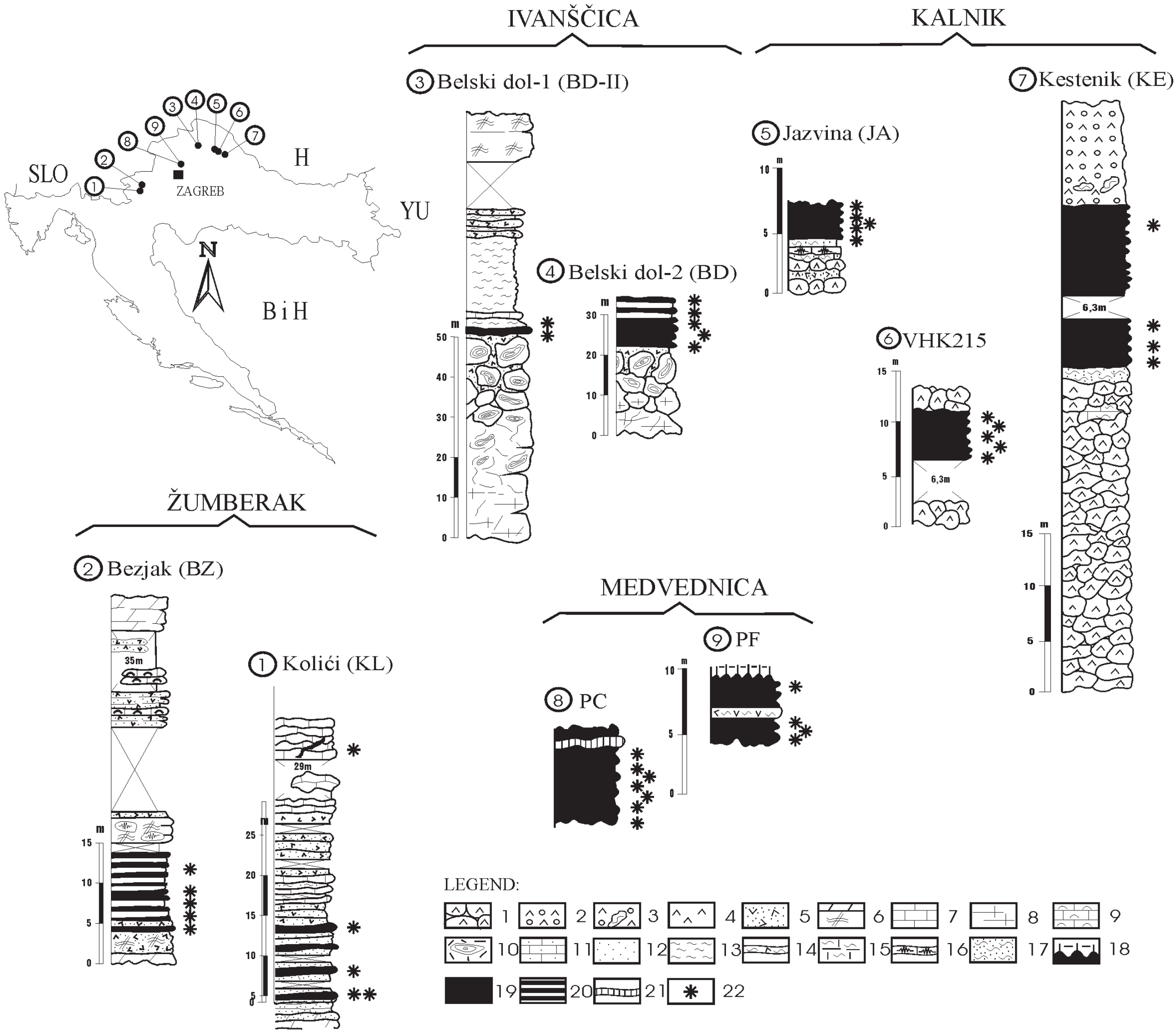

Fig. 2. Detailed geological sections of Žumberak Mt (sections 1 and 2), Ivanščica Mt (sections 3 and 4), Kalnik Mt (sections 5, 6 and 7) and Medvednica Mt (sections 8 and 9). *Legend:* 1 — pillow lava; 2 — metabasalt with amygdaloidal structure; 3 — shale xenolith in metabasalts; 4 — metabasalt, massive; 5 — pyroclastic rocks; 6 — platform dolomite, massive; 7 — limestone, massive; 9 — limestone with Pelecipoda; 10 — limestone with "oncoidal like" structure; 11 — calcarenite; 12 — siltstone; 13 — shale; 14 — tuffitic shale; 15 — calcitized shale; 16 — silicified reddish radiolarian limestone; 17 — silty shale; 18 — marl; 19 — radiolarite; 20 — greenish-gray radiolarian chert interlayered with pyroclastic rock; 21 — Mn-enriched beds; 22 — sample position (time scale see Fig. 9).

ric laminae of microquartz, 0.5 to 1 mm in length. The rock is determined as hematitic radiolarian chert.

The Belski dol-2 section (BD) (4 on Fig. 2). Red radiolarites are overlying brecciated and dolomitized grayish pelecypod limestones. In the lower part of the siliceous interval there are cm- to dm-thick layers of dark red radiolarian chert in alternation with cm-thick layers of mudstones. In the upper part of the package the cherts are greenish. The age of the lower carbonate part is documented with algae and foraminifers (Upper Anisian) and the age of cherts with radiolarians (Lower Ladinian).

All samples from the siliceous interval are determined as radiolarian cherts. The rock matrix is granular microquartz. The radiolarian skeletons are mainly affected by the recrystallization and calcitization processes. The radial chalcedony has been found only in some skeletons. Clastic detritus is represented by quartz and white mica. The accessory minerals are zircon, tourmaline, biotite and opaque mineral grains. The matrix is enriched in ferruginous and manganese substance. Sample 35 is determined as a weakly tuffitic radiolarian chert. The rock matrix is also composed of granular microquartz and mica (sericite?). Accessory minerals are apatite, zircon, and opaque mineral grains. The entire rock is slightly calcitized.

The Jazvina section (JA) (5 on Fig. 2). The lower part of the section is composed of calcitized, weakly porphyric ophitic metabasalts. The pillow lavas are interlayered with light-green basic tuff. The sediments which overlie the effusive rocks are composed of red silty shale and silicified redish radiolarian microsparite in the lower part, and greenish-gray silty radiolarian chert in the upper part. According to radiolarians, the chert is Upper Carnian–Middle Norian.

The silt-sized component of shale is composed of quartz grains, white mica, and subordinate chlorite. The accessory minerals are rounded zircon and apatite. The radiolarian tests in silty cherts are irregularly distributed, and mostly completely recrystallized into microcrystalline quartz.

The VHK section (6 on Fig. 2). The interval of siliceous rocks, from 4.5 to 5 m thick, is intercalated within the pillow lavas. The contact towards the underlying deposits is covered, and towards the overlying deposits it is easily visible. The chert contains Early Ladinian radiolarians.

The lower part of the section is composed of silty radiolarian greenish cherts. The matrix of the rock is composed of microcrystalline quartz, white micas and grains of resorbed quartz. The accessory minerals are apatite, epidote, zircon and opaque mineral grains. In the upper part of the section the silt-clayey component decreases; therefore the rock is mainly composed of radiolarian chert. In the uppermost part of the sedimentary succession there is silicified tuffitic radiolarian shale. The rock matrix consists of microcrystalline quartz with parallel flakes of white mica. The accessory green mineral belongs to the zoisite group.

The Kestenik section (KE) (7 on Fig. 2). Red siliceous rocks are found between underlying pillow lava (ophitic metabasalt) and overlying calcitized vesicular metabasalt. The age of sediments lying directly over the effusives is determined as Middle to Late Carnian, and by the top of the section as Late Carnian.

The lower interval is composed of a green-gray silty siliceous shale. The matrix is made up of clay minerals and crypto- to microcrystalline quartz. The silt-sized components consist of quartz grains, phyllosilicates and feldspars, while rounded zircons, apatite and opaque ferruginous grains are subordinate. The middle and upper part of the sediments are composed of alternating dark red radiolarian cherts with millimetre to centimetre thick interbeds of very thinly laminated silty shales. The matrix of the radiolarian cherts is made up of microcrystalline quartz.

The "PC" and "PF" sections (8 and 9 on Fig. 2). The foot-wall of the reddish radiolarite sequences is unknown, due to intense tectonics (tectonic melánge), while the hanging-wall is represented by disconform Paleocene calcitic siltstones. The radiolarites from "PC" and "PF" sections are assigned to Upper Ladinian or base of Carnian and Upper Carnian.

The matrix of the radiolarite is composed of microcrystalline quartz with millimetre radiolarian enriched laminae, while quartz grains, muscovite/illite, apatite and zircon are accessory. Very small fractures are filled with calcite. Within the "PC" section, Mn-enriched laminae occur from few-millimetre to 2 cm thick. Manganese is probably a consequence of hydrothermal activity during or immediately after volcanic effusion on the sea floor. In the middle part of the "PF" section a bed of green-gray, homogeneous tuffitic radiolarian silty shale has been observed. The matrix is composed of clay minerals, cryptocrystalline quartz and subordinate chlorite. The accessory components include apatite, zircon and hematite.

Analytical methods

For the microscopic analysis thin sections of all radiolarite samples were made (42 in total).

Pieces of chert in all samples with obvious Fe-Mn coatings and calcite veins were hand-picked and removed to avoid the contamination. The remaining samples were powdered in agate mortar. Chemical analysis of the sediments was performed by X-ray fluorescence (XRF). Philips PW 1400 and PW 1480 instruments were used to determine the concentrations of the major and trace elements. The method of sediment analysis was calibrated with 106 international standards and 24 synthetic standards for elements or ranges of concentration not covered by international standards. Analytical precision was better than 2 % for major elements and better than 5 % for trace elements.

Rare earth elements (REE), as well as some of the trace elements which were below the detection limit of XRF analysis, were determined by inductively coupled plasma mass spectrometry (ICP-MS) with SCIEX, model 250, apparatus, following the pressure dissolution in hydrofluoric acid. Analytical precision was better than 5 %. The completeness of dissolution was checked by dissolving and analysing lithium tetraborat/metaborat melt glasses used by XRF.

CO_2 contents were determined in selected samples (Table 1) with indication of carbonate occurrence. We used modified pressure-sensitive method of Klosa (1994). The analytical precision is 1 % if 100 mBar pressure is reached in the reaction vessel.

Results and discussion

The major and trace elements are listed in Table 1 and Table 2. The raw analytical data of major elements were recalculated on a volatile-free basis. The rare earth analytical data and REE ratios were reported in Table 3. The correlation coefficient (r) values for major elements are shown in Table 4. The problem of compositional data (close data) of major elements and the dilution effect of the other elements with SiO_2 was solved by a log-ratio transformation ***log (x/y)*** (Aitchison 1986), with the SiO_2 being used as a denominator for all variables. The same procedure was also used for the trace elements (Aitchison 1986; Swan & Sandilands 1996).

Major elements

The ***silica*** content in all analysed radiolarian cherts is high (>90 % for the majority of the samples; Table 1). On Kalnik Mt it varies from 77 to 97 %, and on Medvednica Mt from 89 to 97 %. In cherts on Žumberak Mt the silica content varies from 77 to 98 % and on Ivanščica Mt from 74 to 92 %. Lower silica content (74 to 79 % SiO_2) and increased content of carbonate (3 to 14 % CaO) was registered in all samples lying closer to the carbonate bedrocks (limestones, dolomites) (Table 1: samples BZ-8, BD-12 and BD-II/4). In the radiolarian cherts on Žumberak Mt (section Bezjak) along with calcium, there is an increas of MgO which indicates the existence of dolomitization processes.

Table 1: Major element data (wt. % — volatile free; CO_2 measurements after Klosa 1994; Stdv = Standard deviation; geomean = geometric mean; $Fe_2O_3* = Fe_{total}$).

	SiO_2	TiO_2	Al_2O_3	Fe_2O_3*	MnO	MgO	CaO	Na_2O	K_2O	P_2O_5	CO_2
Kalnik											
KE-0/98	90.84	0.164	4.44	1.79	0.056	1.31	0.11	0.31	0.95	0.028	
KE-1/98	93.51	0.104	3.08	1.22	0.050	1.10	0.09	0.21	0.61	0.015	
KE-2/98	92.83	0.128	3.45	1.37	0.069	1.16	0.11	0.22	0.67	0.016	
KE-3/98	91.52	0.143	3.86	1.71	0.079	1.63	0.08	0.22	0.74	0.024	
JA-0/98	90.53	0.167	4.69	1.83	0.147	1.24	0.14	0.38	0.88	0.035	
JA-1/98	85.37	0.283	7.91	2.48	0.110	1.47	0.15	0.47	1.71	0.057	
JA-2/98	96.55	0.051	1.70	0.67	0.072	0.32	0.20	0.08	0.33	0.012	
JA-3/98	88.13	0.205	6.12	2.62	0.085	1.04	0.13	0.34	1.28	0.049	
JA-4/98	94.64	0.078	3.09	0.81	0.050	0.44	0.08	0.15	0.64	0.020	
VHK-215	91.87	0.154	3.74	1.52	0.119	0.56	1.07	0.22	0.74	0.018	
VHK-215/1	77.31	0.678	8.20	5.17	0.163	2.06	3.07	0.43	2.69	0.230	1.89
VHK-215/3	93.99	0.092	2.38	0.83	0.139	0.29	1.68	0.15	0.44	0.012	
VHK-215/4	95.63	0.084	1.86	0.66	0.068	0.30	0.85	0.14	0.39	0.018	
VHK-215/5	80.86	0.464	9.74	3.73	0.179	2.41	0.22	0.36	2.00	0.041	
Geomean	**90.09**	**0.155**	**4.02**	**1.57**	**0.091**	**0.88**	**0.25**	**0.24**	**0.83**	**0.027**	
Stdv	**5.60**	**0.173**	**2.49**	**1.28**	**0.044**	**0.67**	**0.87**	**0.12**	**0.69**	**0.056**	
Medvednica											
PF-1	92.06	0.110	3.54	1.24	0.220	1.49	0.56	0.21	0.53	0.035	
PF-5	90.64	0.115	3.28	3.52	0.320	0.64	0.62	0.14	0.68	0.039	
PF-7	91.98	0.141	3.42	2.55	0.176	0.68	0.18	0.22	0.62	0.039	
PF-11	97.44	0.050	1.32	0.25	0.067	0.27	0.28	0.08	0.21	0.020	
PC-2	92.62	0.120	3.18	1.02	0.249	0.65	1.36	0.16	0.63	0.013	
PC-6	89.14	0.209	5.42	2.01	0.179	1.34	0.19	0.38	1.11	0.030	
PC-10	90.93	0.130	4.48	1.48	0.320	1.35	0.16	0.30	0.84	0.018	
PC-14	90.85	0.117	3.95	1.12	0.368	0.98	1.65	0.19	0.77	0.021	
PC-19	94.49	0.104	2.67	1.04	0.118	0.57	0.30	0.17	0.53	0.015	
PC-23	95.24	0.101	2.31	1.00	0.058	0.48	0.09	0.18	0.53	0.021	
PC-24	91.18	0.173	4.44	1.59	0.106	1.14	0.18	0.29	0.88	0.028	
Geomean	**92.39**	**0.118**	**3.26**	**1.28**	**0.169**	**0.78**	**0.33**	**0.20**	**0.62**	**0.024**	
Stdv	**2.41**	**0.041**	**1.13**	**0.89**	**0.107**	**0.41**	**0.52**	**0.08**	**0.23**	**0.009**	
Žumberak											
BZ-8	77.20	0.030	1.06	0.70	0.045	6.88	13.77	0.05	0.24	0.026	14.33
BZ-10	85.88	0.036	1.20	1.01	0.030	4.23	7.24	0.10	0.23	0.025	8.79
BZ-14	95.75	0.025	0.74	0.21	0.019	0.83	2.24	0.06	0.12	0.020	2.55
BZ-33	86.95	0.162	4.13	1.26	0.024	2.64	3.45	0.11	1.23	0.043	4.27
BZ-37	90.40	0.232	5.19	1.37	0.023	0.82	0.36	0.15	1.42	0.042	
KL-13	98.50	0.021	0.67	0.17	0.006	0.02	0.41	0.08	0.12	0.007	
KL-18	96.05	0.035	1.12	0.22	0.010	0.36	1.82	0.10	0.27	0.013	
KL-24A	93.81	0.136	3.09	1.46	0.010	0.36	0.10	0.15	0.86	0.047	
KL-28	93.78	0.101	2.87	1.53	0.018	0.40	0.09	0.14	1.02	0.048	
KL-70	97.37	0.022	0.59	0.17	0.005	0.01	1.61	0.08	0.12	0.016	
Geomean	**91.34**	**0.054**	**1.55**	**0.57**	**0.015**	**0.44**	**1.12**	**0.10**	**0.36**	**0.024**	
Stdv	**6.59**	**0.074**	**1.64**	**0.58**	**0.012**	**2.28**	**4.33**	**0.04**	**0.51**	**0.015**	
Ivanščica											
BD-12	79.51	0.170	4.11	2.73	0.500	0.67	10.99	0.07	1.19	0.057	7.78
BD-16	84.38	0.102	2.25	3.74	1.111	0.39	7.40	0.06	0.51	0.053	5.50
BD-21	92.00	0.155	3.62	1.26	0.176	0.39	1.29	0.12	0.95	0.039	
BD-25	90.32	0.170	3.72	1.30	0.463	0.56	2.36	0.17	0.89	0.046	2.33
BD-35	88.72	0.210	4.54	2.50	0.510	0.70	1.38	0.09	1.31	0.051	
BD-II/4	74.09	0.155	3.66	17.27	0.340	0.57	2.51	0.05	1.28	0.076	1.80
BD-II/4A	85.34	0.104	2.42	4.38	0.631	0.30	5.69	0.09	0.80	0.246	3.83
Geomean	**84.70**	**0.148**	**3.38**	**3.16**	**0.468**	**0.49**	**3.36**	**0.09**	**0.95**	**0.065**	
Stdv	**6.33**	**0.038**	**0.84**	**5.64**	**0.293**	**0.15**	**3.66**	**0.04**	**0.29**	**0.074**	

The Si/Si+Al+Fe ratio (Rangin et al. 1981) was calculated to evaluate the origin of silica in the radiolarian cherts. Because of the increased content of secondary carbonate in cherts, the Si/Si+Al+Fe+Ca ratio (Ruiz-Ortiz et al. 1989) was not used. The values for Si/Si+Al+Fe in the radiolarian cherts of north-western Croatia are higher than values obtained for the Mediterranean cherts (0.8–0.9; Ruiz-Ortiz et al. 1989), and are above 0.91 for the majority of the samples. Although such high values indicate biogenic origin of SiO_2, they also show additional silica enrichment in the radiolarian cherts (from shale in chert/shale couplet) and dilution of the other components during diagenesis. The high negative correlation coefficient between silica and the majority of other major elements indicates the process of dilution especially in cherts on the Kalnik and Medvednica Mts (Table 4). The same process is not so evident in the cherts of Ivanščica Mt, and values of the correlation coefficient, although mostly negative, are not significant. The situation on Žumberak Mt is quite similar to the one on Ivanščica Mt.

Because of the aforementioned diagenetic migration and the dilution effect of the other elements, SiO_2 is inappropriate for paleogeographic consideration of the position of the sedimentary basin during the radiolarian chert genesis (Murray 1994).

Aluminium, titanium and potassium are abundant in clay minerals and aluminosilicates and are good indicators of the clastic and detritic component in sediments (terrigenous input) (Murray 1994). In all analysed radiolarian cherts aluminium, titanium and potassium show a high mutual correlation (Table 4) which is also well defined on the diagram (Fig. 3).

The contents of Al_2O_3 are relatively high in all chert samples. Its highest content was registered on Kalnik Mt (range 1.7 to 9.74 %) in sections "VHK" and "JA" (Table 1). Al_2O_3

Table 2: Trace element data (mg/kg; Stdv = Standard deviation; geomean = geometric mean).

	As	Ba	Co	Cr	Cs	Cu	Ga	Hf	Li	Nb	Ni	Pb	Rb	Sc	Sr	Ta	Th	Tl	U	V	W	Y	Zn	Zr
Kalnik																								
KE-0/98	3.31	81.1	7.2	21.6	2.75	29.4	5.91	1.00	64.5	3.9	19.4	6.1	34.0	4.2	11.5	0.29	3.08	0.220	0.65	21.9	0.52	5.66	48.5	36.6
KE-1/98	2.79	56.9	5.4	14.0	2.23	24.7	3.82	0.53	70.6	2.2	15.4	5.3	23.2	2.3	11.4	0.15	1.85	0.160	0.54	14.5	0.38	2.98	36.2	20.9
KE-2/98	0.03	95.7	4.4	10.7	1.89	24.3	3.59	0.47	15.4	1.9	16.8	3.9	29.8	2.8	8.5	0.13	1.91	0.180	0.38	26.2	0.29	4.08	23.3	18.1
KE-3/98	1.32	67.1	5.6	18.9	2.58	49.5	5.27	0.80	100.0	3.0	21.5	3.0	27.8	3.2	9.4	0.22	2.72	0.180	0.82	21.5	0.47	3.85	43.2	30.6
JA-0/98	1.57	109.0	11.5	26.1	2.69	65.3	6.29	0.98	29.6	3.9	31.5	23.8	37.8	5.0	9.9	0.28	3.98	0.240	0.53	29.4	0.90	9.39	67.3	36.1
JA-1/98	0.78	179.0	14.3	35.6	4.33	104.0	9.67	1.70	21.3	6.5	43.8	3.0	53.8	7.5	10.9	0.50	6.53	0.460	0.78	42.0	0.93	11.20	57.0	59.7
JA-2/98	0.28	54.5	2.8	9.6	1.04	15.4	2.17	0.28	12.7	1.1	10.7	3.7	14.0	1.2	6.4	0.08	1.16	0.110	0.45	6.9	0.29	2.94	14.5	10.2
JA-3/98	1.35	147.0	10.8	27.3	3.66	16.2	7.34	1.20	18.4	5.0	40.6	21.5	55.5	5.7	8.9	0.36	4.95	0.350	0.66	25.1	1.03	8.47	64.7	42.9
JA-4/98	1.64	62.2	4.8	16.9	2.31	23.1	4.24	0.65	74.8	2.6	18.4	4.2	24.4	2.5	9.5	0.21	2.27	0.210	0.71	17.9	0.50	3.72	34.1	23.3
VHK-215	2.44	75.8	4.2	18.0	3.48	27.3	5.16	0.89	57.0	3.2	11.8	7.0	31.3	3.2	15.8	0.24	2.57	0.190	1.02	20.1	0.61	6.22	37.7	31.0
VHK-215/1	4.30	119.0	8.6	63.2	8.54	39.9	10.80	1.93	41.3	10.8	33.9	7.8	77.6	11.0	25.7	0.72	3.21	0.360	0.54	64.9	1.49	16.10	51.8	77.9
VHK-215/3	2.04	47.0	2.4	13.2	1.83	16.3	2.93	0.57	60.5	1.9	6.7	3.9	18.2	1.8	13.6	0.14	1.63	0.120	0.43	11.1	0.40	5.38	28.1	21.3
VHK-215/4	1.44	43.5	2.5	9.7	1.58	12.1	2.48	0.63	57.3	2.4	9.6	3.3	15.4	1.5	10.5	0.20	1.77	0.110	0.38	11.2	0.35	4.68	30.6	22.7
VHK-215/5	3.15	171.0	14.7	60.3	10.20	36.9	12.90	2.26	62.4	8.8	46.6	4.5	70.8	10.3	22.0	0.66	6.62	0.460	2.60	57.8	1.41	13.00	83.2	80.6
Geomean	**1.26**	**84.3**	**6.0**	**20.4**	**2.88**	**28.8**	**5.15**	**0.85**	**41.1**	**3.4**	**19.8**	**5.6**	**32.1**	**3.6**	**11.6**	**0.25**	**2.77**	**0.214**	**0.65**	**22.1**	**0.59**	**6.03**	**40.3**	**31.3**
Stdv	**1.20**	**45.4**	**4.2**	**17.4**	**2.65**	**24.8**	**3.25**	**0.59**	**26.3**	**2.8**	**13.4**	**6.7**	**20.2**	**3.2**	**5.4**	**0.20**	**1.76**	**0.121**	**0.56**	**17.2**	**0.40**	**4.08**	**19.0**	**21.8**
Medvednica																								
PF-1	0.51	66.7	6.2	12.3	1.59	27.7	4.27	0.58	57.5	2.4	17.1	2.6	22.7	2.9	21.5	0.19	2.05	0.140	0.46	16.7	0.44	5.17	33.8	21.6
PF-5	1.00	62.5	7.6	9.4	1.16	20.9	3.24	0.52	41.3	2.3	19.4	12.0	16.0	1.4	25.7	0.15	1.91	0.120	0.78	26.1	0.54	3.17	25.1	19.9
PF-7	13.60	93.4	5.5	15.2	2.79	33.9	4.74	0.82	42.1	3.6	17.0	4.7	33.1	3.1	25.5	0.26	2.63	0.290	0.86	15.6	0.98	5.15	30.3	30.4
PF-11	1.34	27.6	1.4	8.2	0.41	13.8	1.43	0.34	22.2	2.4	6.3	1.5	7.1	0.8	14.1	0.10	0.95	0.058	1.79	20.3	0.25	1.86	10.3	13.2
PC-2	2.91	70.9	6.8	14.8	1.71	58.2	4.04	0.70	35.6	2.8	10.6	3.5	27.8	2.5	17.7	0.21	2.25	0.200	0.89	20.2	0.91	3.71	25.2	24.0
PC-6	31.30	99.8	17.6	14.2	2.97	33.8	6.22	1.44	29.9	5.4	16.6	6.1	39.1	3.5	21.6	0.49	4.96	0.370	1.31	20.6	2.18	7.22	36.9	44.2
PC-10	19.10	76.9	17.7	15.8	2.08	28.1	4.73	0.91	37.5	3.2	23.2	3.5	29.9	2.1	16.8	0.27	3.35	0.270	0.90	9.7	4.07	3.64	31.2	28.7
PC-14	10.80	85.7	5.1	9.1	1.88	26.1	4.47	0.76	34.5	3.7	11.8	4.7	28.2	2.3	19.6	0.25	2.31	0.250	0.73	12.8	0.84	4.62	28.2	27.5
PC-19	10.10	60.0	3.7	9.5	1.43	23.8	2.94	0.65	30.2	2.8	12.2	4.7	21.4	1.9	18.2	0.20	2.07	0.190	0.81	11.9	0.93	3.79	22.2	22.2
PC-23	8.26	63.4	3.2	9.8	1.30	24.1	2.60	0.65	24.0	2.1	10.4	4.8	19.5	1.6	15.8	0.17	1.85	0.160	1.05	11.4	0.76	3.58	17.8	21.1
PC-24	2.96	94.7	7.2	15.1	2.23	28.7	5.08	1.11	30.0	3.7	21.0	6.1	34.2	3.1	18.4	0.31	3.11	0.260	0.88	17.7	0.93	5.94	37.5	36.5
Geomean	**4.94**	**69.4**	**6.0**	**11.8**	**1.60**	**27.4**	**3.73**	**0.72**	**33.8**	**3.0**	**14.1**	**4.3**	**23.3**	**2.1**	**19.2**	**0.22**	**2.31**	**0.189**	**0.90**	**16.0**	**0.88**	**4.11**	**25.7**	**25.1**
Stdv	**9.45**	**20.6**	**5.4**	**3.0**	**0.73**	**11.2**	**1.33**	**0.30**	**9.8**	**0.9**	**5.2**	**2.7**	**9.2**	**0.8**	**3.7**	**0.10**	**1.04**	**0.089**	**0.35**	**5.0**	**1.08**	**1.47**	**8.2**	**8.6**
Žumberak																								
BZ-8	0.07	14.8	0.4	4.7	0.64	6.9	0.81	0.28	21.6	0.4	3.8	1.6	7.3	0.8	26.4	0.11	0.56	0.096	0.91	12.2	0.08	5.40	11.9	6.8
BZ-10	0.75	15.6	1.5	13.6	0.51	16.6	1.22	0.23	30.0	0.6	23.1	2.2	5.9	0.7	15.3	0.07	0.68	0.089	1.67	4.6	0.11	3.43	11.4	8.4
BZ-14	0.47	12.1	1.1	3.0	0.18	9.0	0.64	0.15	11.5	0.4	2.5	8.4	3.1	0.5	3.2	0.04	0.43	0.040	0.62	4.3	0.09	3.22	11.6	4.9
BZ-33	0.73	61.1	3.8	23.8	2.47	23.4	4.55	0.94	22.9	3.0	12.3	26.5	36.7	3.9	19.4	0.28	3.05	0.180	0.79	30.1	0.54	8.76	50.8	30.5
BZ-37	6.50	96.5	3.8	28.0	3.41	22.9	6.57	1.47	41.4	4.6	15.8	9.9	43.8	4.8	24.4	0.36	4.14	0.250	0.89	35.5	0.72	8.93	39.5	52.5
KL-13	0.32	15.9	0.7	6.0	0.24	3.5	0.73	0.11	16.0	0.4	3.6	4.9	3.1	0.6	0.6	0.03	0.34	0.062	0.97	3.3	0.40	1.47	40.8	4.3
KL-18	0.93	17.4	0.4	3.1	0.64	11.9	1.66	0.20	40.6	0.6	1.5	179	6.1	0.6	6.6	0.05	0.57	0.044	0.64	4.1	0.14	2.76	310	6.8
KL-24A	0.54	61.5	2.3	14.2	2.63	33.8	3.77	0.76	37.0	2.5	8.3	3.8	27.8	2.3	24.1	0.18	2.19	0.130	0.66	22.8	0.45	10.20	19.8	26.7
KL-28	0.81	54.5	1.6	10.1	1.91	29.4	3.33	0.52	43.0	1.6	6.4	4.5	24.9	2.7	21.2	0.13	1.53	0.099	0.82	19.4	0.30	10.30	21.3	18.9
KL-70	0.80	12.4	0.1	1.8	0.20	2.8	1.10	0.13	11.0	0.7	1.6	8.7	3.0	0.2	1.6	0.03	0.44	0.028	0.95	2.6	0.25	6.34	6.2	7.7
Geomean	**0.65**	**26.8**	**1.0**	**7.6**	**0.77**	**12.0**	**1.78**	**0.33**	**24.6**	**1.0**	**5.4**	**7.9**	**9.8**	**1.1**	**8.6**	**0.09**	**0.95**	**0.083**	**0.86**	**9.1**	**0.24**	**5.13**	**25.2**	**11.8**
Stdv	**1.88**	**29.9**	**1.3**	**9.1**	**1.20**	**11.0**	**2.02**	**0.45**	**12.6**	**1.4**	**7.1**	**54.6**	**15.6**	**1.6**	**10.3**	**0.11**	**1.32**	**0.069**	**0.30**	**12.3**	**0.22**	**3.30**	**91.8**	**15.7**
Ivanščica																								
BD-12	1.45	55.6	2.3	12.4	3.71	21.6	3.85	1.02	10.7	2.9	17.6	41.2	37.8	3.5	27.5	0.26	3.53	0.180	0.50	21.2	4.08	14.80	53.2	32.9
BD-16	16.40	66.7	2.3	5.7	1.87	55.7	2.38	0.64	12.1	1.9	20.3	130	19.0	2.3	37.2	0.15	1.95	0.090	0.35	45.9	1.40	24.80	30.6	26.4
BD-21	3.17	65.9	4.2	10.1	2.86	26.7	4.40	1.18	13.2	3.5	16.1	12.8	34.6	2.7	10.3	0.24	3.09	0.190	1.07	23.1	0.86	14.20	32.8	56.4
BD-25	5.61	115	3.4	14.1	2.88	16.1	4.34	0.97	14.6	3.8	11.4	8.1	35.0	3.0	28.1	0.27	3.26	0.190	0.98	24.1	1.28	14.20	30.2	38.8
BD-35	29.30	90.3	4.7	26.8	4.59	72.1	6.26	1.30	18.1	4.7	37.8	16.0	58.3	5.3	15.1	0.32	3.80	0.220	0.73	32.6	1.25	16.30	40.2	60.9
BD-II/4	4.32	77.6	6.9	13.9	2.88	155.0	6.12	1.33	15.6	5.0	74.4	26.3	62.8	4.8	22.5	0.26	3.30	0.250	0.83	70.3	10.3	22.10	161.0	82.8
BD-II/4A	3.80	51.0	7.8	7.9	1.67	57.3	2.90	0.67	9.4	2.2	43.2	18.1	34.9	2.7	36.7	0.16	2.17	0.200	0.35	59.4	1.04	32.20	44.7	27.8
Geomean	**5.73**	**72.0**	**4.1**	**11.7**	**2.77**	**44.2**	**4.10**	**0.98**	**13.09**	**3.2**	**26.0**	**23.7**	**37.8**	**3.3**	**23.3**	**0.23**	**2.94**	**0.181**	**0.63**	**35.7**	**1.88**	**18.89**	**46.4**	**42.9**
Stdv	**10.15**	**22.1**	**2.2**	**6.8**	**1.01**	**47.7**	**1.47**	**0.28**	**2.99**	**1.2**	**22.3**	**42.8**	**15.2**	**1.1**	**10.2**	**0.06**	**0.69**	**0.049**	**0.29**	**19.5**	**3.45**	**6.88**	**47.0**	**20.9**

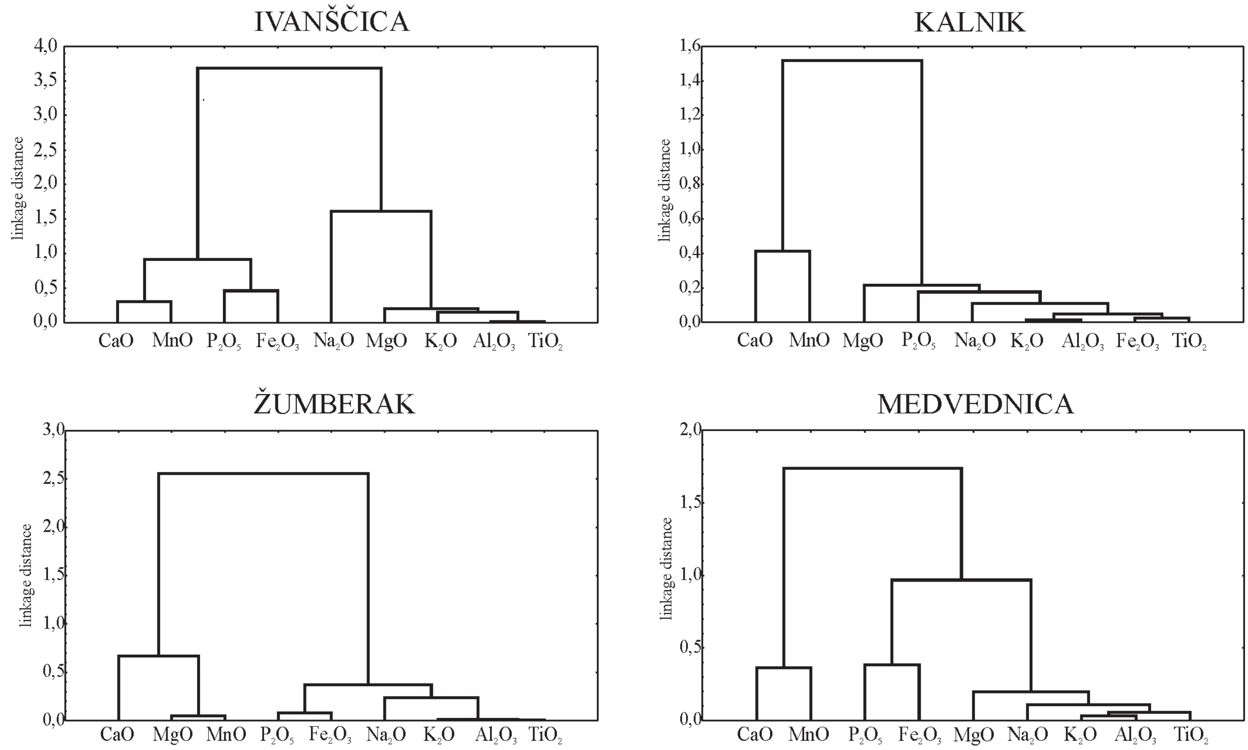

Fig. 3. Cluster analysis diagrams of major elements (Tree clustering; Linkage rule = Ward's method; Distance measure = 1-Pearson r).

in those samples is mainly connected to the white mica, clay minerals? and epidote-coisite mineral group. The radiolarian cherts on the Medvednica and Ivanščica Mts have approximately the same content of Al_2O_3. On Žumberak Mt, the content of aluminium is the lowest except for two samples, which were microscopically determined as clayey radiolarian cherts. Similar to the TiO_2 the aluminium is positively correlated with elements which mainly originated from the detritic component.

TiO_2 is mostly contained in the heavy mineral fraction. Its content in the Kalnik, Medvednica and Ivanščica Mts radiolarian cherts is more or less equal, and ranges between 0.05 and 0.67 %, while it is lower on Žumberak Mt and ranges between 0.02 and 0.23 %. TiO_2 on Žumberak Mt shows a very high correlation to Al_2O_3 and K_2O and a high correlation to Na_2O. All these elements are, like titanium, connected to the detritic component in the radiolarian cherts. Similar values of the correlation coefficients to the same elements were obtained for the cherts on the Kalnik and Medvednica Mts. On Ivanščica Mt TiO_2 shows a high positive correlation only to Al_2O_3, and lower correlations to K_2O and MgO.

K_2O content in the analysed rocks varies from 0.12 to 2.69 %. The highest contents were registered in the Kalnik radiolarian cherts (section VHK). Potassium is, like aluminium, mainly connected to aluminosilicates (white micas) and is a part of the clastic component.

Iron and phosphorus. Increased iron contents can indicate a strong hydrothermal influence during sedimentation. In this case the iron content decreases with distance from the spreading ridge.

The content of iron is highest in the Ivanščica Mt radiolarian cherts (max. value 17.27 %), while it is significantly lower on the Kalnik and Medvednica Mts (Table 1). The lowest values of Fe are registered in the Žumberak cherts. In sample KL-70 (Žumberak Mt) a portion of Fe can also be found in veins along with calcite.

The increased content of iron on Ivanščica Mt is not followed by an increase of aluminium which is an indicator of its hydrothermal origin. The REE spectra also support the conclusion that the hydrothermal iron has been precipitated from seawater.

The iron on Kalnik Mt shows a very high correlation to TiO_2, and a high correlation to K_2O, Al_2O_3 and Na_2O (Fig. 3; Table 4) which indicates that part of the iron in the radiolarian cherts is also connected to the terrigenous material. In the other three investigated areas the Fe shows high correlation to the phosphorus.

The phosphorus content on the Kalnik, Medvednica and Žumberak sections is relatively uniform and low, while it is increased only in Ivanščica radiolarian cherts (Table 1). The relatively low contents were conditioned by diagenetic SiO_2 dilution or silicification. The origin of phosphorus in these rocks is not clear and could be equivocal. The first possibility is that the phosphorus is of biogenic origin, and the other is that the phosphate from seawater was adsorbed onto ferric hydroxide which was precipitated from the hydrothermal fluids on the divergent plate margins (Berner 1973) (the content of Fe on Ivanščica Mt rises up to 17 %!). During diagenesis the phosphate is transformed to apatite which is hard to distinguish from the biogenic type. Biogenic apatite has a higher content of Sc, Y, La, and REE (Marchig et al. 1982). The consideration of the contents of the aforementioned elements on the studied sections shows that the content of Y, La and ΣREE is almost two times higher on Ivanščica Mt than on the Kalnik, Medved-

Table 3: Rare earth contents (mg/kg) and Rare earth ratios (Normalization: NASC = North American shale composit; Gromet et al. 1984).

	La	Ce	Pr	Nd	Sm	Eu	Gd	Tb	Dy	Ho	Er	Tm	Yb	Lu	Sum (Σ)	(La/Yb)n n=NASC	Ce/Ce* n=NASC
Kalnik																	
KE-0/98	8.7	19.40	1.88	6.65	1.22	0.25	1.16	0.18	0.98	0.20	0.59	0.088	0.57	0.092	**41.96**	1.53	1.17
KE-1/98	5.0	12.20	1.03	3.60	0.62	0.13	0.59	0.09	0.50	0.11	0.32	0.045	0.32	0.054	**24.65**	1.56	1.32
KE-2/98	4.2	15.10	1.06	4.20	0.89	0.19	0.89	0.14	0.72	0.14	0.42	0.057	0.36	0.061	**28.39**	1.17	1.65
KE-3/98	5.0	13.70	1.14	4.03	0.73	0.16	0.73	0.12	0.65	0.13	0.42	0.063	0.41	0.072	**27.36**	1.22	1.40
JA-0/98	8.9	31.10	2.22	8.45	1.89	0.42	1.92	0.29	1.71	0.34	0.95	0.140	0.86	0.140	**59.35**	1.04	1.65
JA-1/98	14.9	48.20	3.75	13.90	2.86	0.65	2.83	0.42	2.17	0.42	1.24	0.180	1.13	0.200	**92.85**	1.32	1.54
JA-2/98	2.5	8.05	0.59	2.21	0.47	0.12	0.56	0.10	0.56	0.11	0.31	0.043	0.26	0.041	**15.88**	0.96	1.57
JA-3/98	10.7	34.70	2.59	9.71	1.95	0.41	1.92	0.29	1.65	0.32	0.95	0.150	0.88	0.150	**66.37**	1.22	1.56
JA-4/98	4.7	13.50	1.17	4.33	0.81	0.16	0.81	0.12	0.65	0.13	0.39	0.060	0.39	0.063	**27.26**	1.21	1.37
VHK-215	8.4	18.00	1.94	7.26	1.48	0.26	1.46	0.21	1.15	0.23	0.65	0.094	0.59	0.099	**41.79**	1.43	1.06
VHK-215/1	14.3	29.80	3.64	14.50	3.08	0.81	3.34	0.51	2.88	0.57	1.62	0.230	1.32	0.210	**76.81**	1.08	0.95
VHK-215/3	5.0	11.10	1.17	4.43	0.99	0.20	1.08	0.18	1.02	0.19	0.52	0.073	0.45	0.071	**26.46**	1.11	1.08
VHK-215/4	5.0	12.90	1.26	4.82	1.00	0.21	1.04	0.16	0.85	0.17	0.45	0.063	0.37	0.062	**28.33**	1.35	1.21
VHK-215/5	17.6	37.80	4.00	14.70	2.73	0.57	2.65	0.41	2.35	0.47	1.40	0.210	1.35	0.230	**86.47**	1.31	1.08
Geomean	**7.1**	**19.01**	**1.68**	**6.27**	**1.26**	**0.27**	**1.28**	**0.20**	**1.09**	**0.22**	**0.63**	**0.092**	**0.57**	**0.095**	**39.73**	**1.24**	**1.31**
Stdv	**4.64**	**12.23**	**1.13**	**4.30**	**0.88**	**0.22**	**0.90**	**0.13**	**0.76**	**0.15**	**0.43**	**0.06**	**0.38**	**0.06**	**25.53**		
Medvednica																	
PF-1	6.2	16.10	1.51	5.65	1.15	0.27	1.10	0.17	0.91	0.17	0.51	0.070	0.41	0.072	**34.29**	1.51	1.25
PF-5	3.4	7.72	0.81	3.06	0.63	0.15	0.61	0.10	0.52	0.11	0.34	0.055	0.36	0.064	**17.88**	0.95	1.10
PF-7	6.6	16.20	1.59	6.07	1.28	0.25	1.19	0.18	0.97	0.20	0.55	0.080	0.51	0.082	**35.72**	1.30	1.17
PF-11	3.2	9.04	0.69	2.45	0.45	0.10	0.43	0.07	0.35	0.07	0.20	0.030	0.18	0.033	**17.29**	1.78	1.48
PC-2	5.0	10.90	1.13	4.16	0.84	0.16	0.77	0.12	0.65	0.14	0.39	0.059	0.38	0.064	**24.74**	1.32	1.10
PC-6	12.0	24.60	2.63	9.41	1.80	0.35	1.74	0.27	1.45	0.29	0.88	0.130	0.83	0.140	**56.52**	1.45	1.06
PC-10	5.1	11.30	1.32	4.79	0.82	0.16	0.83	0.13	0.66	0.14	0.41	0.066	0.42	0.073	**26.21**	1.22	1.05
PC-14	5.0	14.00	1.44	5.61	1.23	0.25	1.22	0.18	0.98	0.19	0.50	0.070	0.44	0.070	**31.20**	1.14	1.21
PC-19	5.5	13.70	1.41	5.35	1.12	0.21	1.09	0.16	0.83	0.17	0.45	0.068	0.41	0.064	**30.52**	1.34	1.16
PC-23	4.4	11.80	1.21	4.53	0.94	0.19	0.91	0.14	0.75	0.15	0.41	0.060	0.38	0.063	**25.95**	1.16	1.21
PC-24	7.4	18.90	1.97	7.47	1.49	0.31	1.49	0.21	1.16	0.22	0.63	0.092	0.59	0.098	**42.03**	1.26	1.17
Geomean	**5.4**	**13.33**	**1.34**	**5.00**	**1.00**	**0.21**	**0.97**	**0.15**	**0.79**	**0.16**	**0.45**	**0.067**	**0.42**	**0.071**	**29.37**	**1.29**	**1.17**
Stdv	**2.41**	**4.81**	**0.53**	**1.94**	**0.39**	**0.08**	**0.38**	**0.06**	**0.31**	**0.06**	**0.17**	**0.02**	**0.16**	**0.03**	**11.20**		
Žumberak																	
BZ-8	6.6	8.85	1.39	5.32	0.96	0.24	1.02	0.15	0.85	0.17	0.46	0.061	0.38	0.059	**26.49**	1.74	0.69
BZ-10	3.9	4.72	0.91	3.57	0.68	0.15	0.71	0.10	0.57	0.11	0.31	0.042	0.23	0.038	**16.01**	1.70	0.58
BZ-14	3.3	5.14	0.76	3.10	0.55	0.12	0.63	0.09	0.48	0.10	0.28	0.040	0.25	0.041	**14.90**	1.32	0.74
BZ-33	14.4	21.30	3.89	14.90	2.70	0.54	2.45	0.34	1.68	0.32	0.91	0.130	0.76	0.120	**64.44**	1.90	0.67
BZ-37	13.0	20.70	3.29	12.50	2.39	0.47	2.16	0.30	1.61	0.32	0.93	0.130	0.82	0.130	**58.75**	1.59	0.75
KL-13	3.3	4.06	0.82	3.05	0.54	0.11	0.48	0.07	0.30	0.05	0.16	0.020	0.14	0.025	**13.16**	2.36	0.59
KL-18	3.2	4.81	0.82	3.11	0.55	0.15	0.56	0.08	0.45	0.09	0.25	0.034	0.20	0.032	**14.30**	1.60	0.70
KL-24A	29.4	25.30	5.54	18.90	3.39	0.68	3.04	0.42	2.02	0.36	0.99	0.130	0.74	0.120	**91.03**	3.98	0.49
KL-28	37.4	26.80	7.46	24.50	4.73	0.95	3.82	0.52	2.33	0.39	1.02	0.130	0.77	0.110	**110.9**	4.86	0.41
KL-70	1.5	1.81	0.46	2.03	0.46	0.09	0.61	0.10	0.64	0.16	0.46	0.066	0.42	0.073	**8.916**	0.43	0.37
Geomean	**7.0**	**8.62**	**1.66**	**6.30**	**1.18**	**0.25**	**1.16**	**0.16**	**0.87**	**0.17**	**0.48**	**0.065**	**0.39**	**0.064**	**28.38**	**1.80**	**0.58**
Stdv	**12.41**	**9.92**	**2.43**	**8.04**	**1.51**	**0.30**	**1.22**	**0.17**	**0.74**	**0.13**	**0.34**	**0.05**	**0.27**	**0.04**	**36.94**		
Ivanščica																	
BD-12	17.4	25.50	4.86	19.30	3.81	0.79	3.97	0.57	3.00	0.58	1.55	0.200	1.26	0.200	**82.99**	1.38	0.64
BD-16	19.0	13.10	4.91	20.60	4.55	1.05	5.30	0.81	4.83	0.97	2.61	0.360	2.09	0.320	**80.50**	0.91	0.30
BD-21	23.0	28.00	6.16	24.60	5.13	0.94	4.96	0.67	3.29	0.60	1.51	0.190	1.13	0.180	**100.4**	2.04	0.54
BD-25	17.5	22.80	4.60	18.40	3.67	0.71	3.74	0.52	2.80	0.55	1.47	0.200	1.26	0.200	**78.42**	1.39	0.58
BD-35	22.4	25.60	4.90	19.10	3.64	0.76	3.82	0.55	3.02	0.60	1.69	0.240	1.49	0.230	**88.04**	1.51	0.57
BD-II/4	61.8	58.60	12.80	49.00	8.85	1.70	8.20	1.05	4.96	0.92	2.68	0.390	2.61	0.430	**213.99**	2.37	0.49
BD-II/4A	20.0	12.50	5.26	24.10	5.70	1.39	7.05	1.02	5.68	1.11	2.93	0.390	2.27	0.360	**89.76**	0.88	0.26
Geomean	**23.26**	**23.53**	**5.81**	**23.58**	**4.81**	**1.00**	**5.07**	**0.71**	**3.80**	**0.73**	**1.98**	**0.268**	**1.65**	**0.261**	**98.34**	**1.41**	**0.46**
Stdv	**15.99**	**15.40**	**2.95**	**10.86**	**1.85**	**0.37**	**1.73**	**0.22**	**1.18**	**0.23**	**0.64**	**0.09**	**0.59**	**0.10**	**48.67**		

nica and Žumberak Mts. The Ivanščica radiolarian cherts show a high correlation of phosphorus only to Y, while there is no correlation to Sc, La and ΣREE. Based on that, and also on the explicit correlation of P to Fe on Kalnik, Medvednica, Žumberak Mts and indirectly on Ivanščica Mt (Fig. 3; Table 4), it can be concluded that the phosphorus in the analysed Triassic radiolarian cherts is mostly bound to hydrothermaly supplied iron.

Calcium, magnesium and manganese. The carbonate content in the Kalnik and Medvednica radiolarian cherts is relatively low (Table 1). The higher content in a few samples is the consequence of secondary calcite which appears in the form of submillimetre veins. CaO shows correlation to Mn on Medvednica, while on Žumberak it also correlates to MgO (Fig. 3; Table 4). There is a highly negative correlation to silica on Žumberak Mt (Table 4), which is mainly the result of diagenetic silicification of carbonate mud. The MgO content on Kalnik and Medvednica Mts is low (Table 1). The slightly increased magnesium contents in samples VHK-215/1 and 215/5 (2.06 and 2.41 % respectively) can originate from the epidote-coisite mineral group. Contrary to that, the calcium and magnesium contents on Žumberak and Ivanščica Mts are significantly higher, especially in the "BZ" section (see Table 1). The high content of those elements in these sections is the result of the dolomitization of the radiolarian cherts that lie closer to the dolomite bedrock. The significantly lower MgO content on Ivanščica Mt is caused by limestones and carbonate breccia that underlie the cherts. The CaO content is significantly higher for the same reason.

Manganese content is relatively low in the cherts with the exception of some Ivanščica samples (Table 1). Although there were layers enriched by manganese oxide found in one

Table 4: Correlation coefficient (r) values for major elements (significant correlations at $p<0.05$; Kalnik: $-0.54<r>0.54$; Medvednica: $-0.63<r>0.63$; Žumberak: $-0.75<r>0.75$; Ivanščica: $-0.77<r>0.77$; (–) indicates negative correlation; $Fe_2O_3^* = Fe_{total}$).

Kalnik										
	SiO_2	**TiO_2**	**Al_2O_3**	**$Fe_2O_3^*$**	**MnO**	**MgO**	**CaO**	**Na_2O**	**K_2O**	**P_2O_5**
SiO_2	1.00									
TiO_2	-0.97	1.00								
Al_2O_3	-0.95	0.86	1.00							
$Fe_2O_3^*$	-0.98	0.98	0.90	1.00						
MnO	-0.71	0.70	0.65	0.66	1.00					
MgO	-0.86	0.79	0.86	0.84		1.00				
CaO	-0.44	0.59					1.00			
Na_2O	-0.84	0.74	0.88	0.80	0.55	0.77		1.00		
K_2O	-0.99	0.97	0.94	0.98	0.64	0.81		0.84	1.00	
P_2O_5	-0.80	0.88	0.60	0.85		0.54	0.75	0.60	0.84	1.00
Medvednica										
	SiO_2	**TiO_2**	**Al_2O_3**	**$Fe_2O_3^*$**	**MnO**	**MgO**	**CaO**	**Na_2O**	**K_2O**	**P_2O_5**
SiO_2	1.00									
TiO_2	-0.82	1.00								
Al_2O_3	-0.93	0.91	1.00							
$Fe_2O_3^*$	-0.65			1.00						
MnO	-0.66				1.00					
MgO	-0.74	0.63	0.84			1.00				
CaO					0.64		1.00			
Na_2O	-0.73	0.91	0.91			0.79		1.00		
K_2O	-0.90	0.93	0.96			0.69		0.89	1.00	
P_2O_5				0.76						1.00
Žumberak										
	SiO_2	**TiO_2**	**Al_2O_3**	**$Fe_2O_3^*$**	**MnO**	**MgO**	**CaO**	**Na_2O**	**K_2O**	**P_2O_5**
SiO_2	1.00									
TiO_2		1.00								
Al_2O_3		0.99	1.00							
$Fe_2O_3^*$		0.78	0.82	1.00						
MnO	-0.96				1.00					
MgO	-0.96				0.93	1.00				
CaO	-0.88				0.86	0.97	1.00			
Na_2O		0.80	0.79	0.79				1.00		
K_2O		0.97	0.99	0.85				0.81	1.00	
P_2O_5		0.80	0.83	0.96				0.75	0.87	1.00
Ivanščica										
	SiO_2	**TiO_2**	**Al_2O_3**	**$Fe_2O_3^*$**	**MnO**	**MgO**	**CaO**	**Na_2O**	**K_2O**	**P_2O_5**
SiO_2	1.00									
TiO_2		1.00								
Al_2O_3		0.98	1.00							
$Fe_2O_3^*$	-0.82			1.00						
MnO					1.00					
MgO		0.87	0.88			1.00				
CaO							1.00			
Na_2O	0.77							1.00		
K_2O		0.81	0.87			0.78			1.00	
P_2O_5										1.00

section on Medvednica Mt (Halamić & Goričan 1995), its content in the radiolarian chert beds is relatively low as a result of its diagenetic migration, and accumulation in centimeter thick layers which were avoided by sampling. This element shows connection only to calcium in all sections, and also to magnesium on Žumberak Mt (Fig. 3). But it shows significant negative correlation to SiO_2 in almost all sections and that indicates its replacement by silica, so that its use as a paleogeographical indicator is questionable (Murray 1994).

Trace elements

Comparing the contents of particular trace elements of analysed radiolarian cherts to recent oceanic radiolarian oozes (Gundlach & Marchig 1982; Marchig et al. 1982, 1986, 1987; Murray et al. 1992b) it is evident that the majority of the values in the cherts are significantly lower than in recent radiolarian oozes. The decreased contents in the studied cherts are the result of an enrichment in SiO_2. Besides that, during the silicification of carbonate sediments, for example, the Ba and Sr were removed from the host sediment (Murray 1994). Because of that effect, the Ba, Sr, V and Co contents do not correspond to the primary contents and should be considered with caution.

Cr, Zr, Hf, Rb, Th and in part V, and major elements Al, Ti and K are mainly incorporated in the detritic and clastic component of the sediment. Their increased content indicates a more intense terrigenous input. However, Cr can be partly mobile and enriched in the hydrothermal precipitates (Marchig et al. 1982). In all analysed radiolarian cherts Cr shows a high or relatively high correlation to the other aforementioned elements, and this shows that it is mainly bound to the terrigenous component.

Individual diagrams for the Žumberak, Ivanščica, Kalnik and Medvednica Mts on the basis of Pearson's correlation coefficient were constructed to understand the relationships and mutual connections between major and trace elements.

Ivanščica Mt. The trace elements on the diagram are separated into two groups (Fig. 4). The first one consists of Zr, Hf, Th, Cr, Rb, Sc and Nb which are characteristic of the terrigenous input in the form of detritic component, as is also proved by the stronger correlations of the named elements to Al_2O_3,

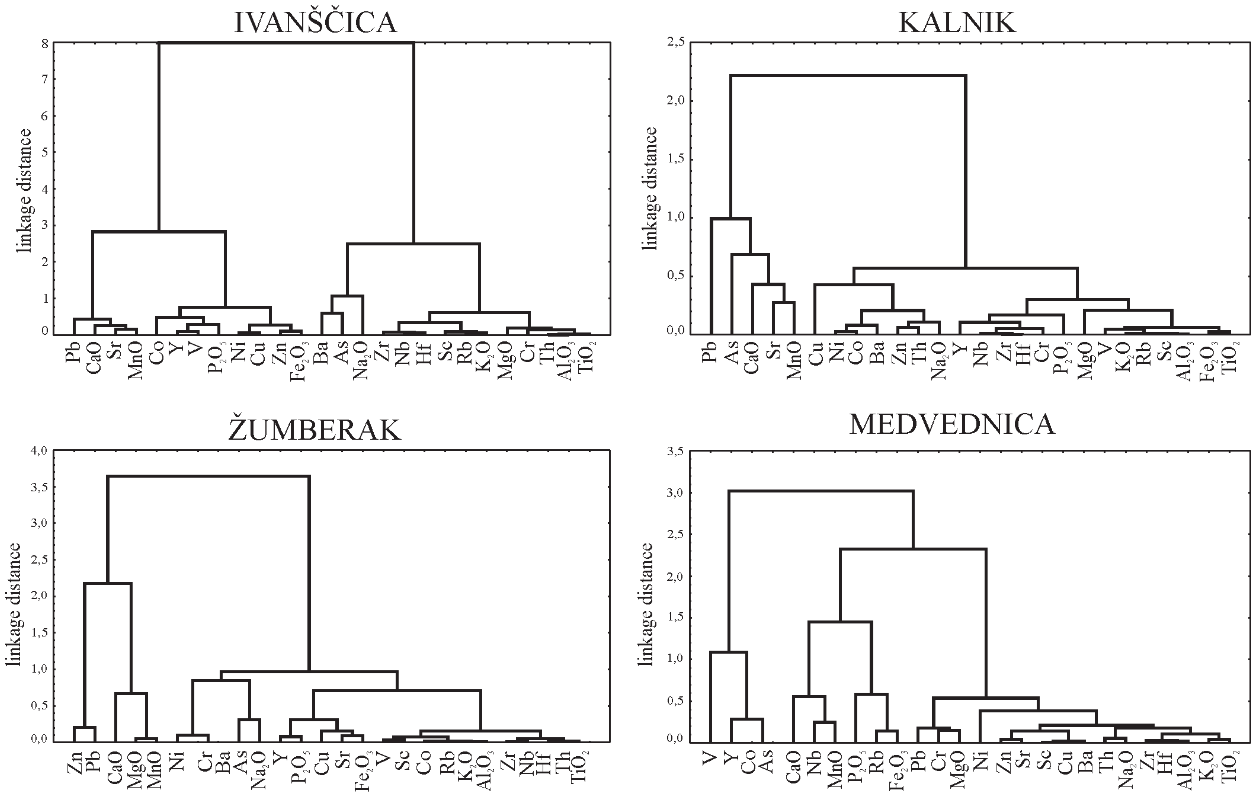

Fig. 4. Cluster analysis diagrams of major and trace elements (Tree clustering; Linkage rule = Ward's method; Distance measure = 1-Pearson r).

TiO_2 and K_2O. The same group of trace elements is less strongly correlated to Ba and As which correlate positively to Na_2O, which means that Ba and As are, at the least, in part of terrigenous origin. The second group consists of Cu, Zn, Ni, Co, V and Y, which represent the hydrothermal component, and correlate positively to major elements such as Fe and P. The connection of Sr and Pb to Mn and Ca is the result of diagenetic processes.

Kalnik Mt. In this area, similar as on Ivanščica, the trace and major elements characteristic of the terrigenous source are separated in two groups with the difference that the iron, phosphorus, sodium and magnesium are in greater part contained in the detritic component (Fig. 4). The second group consists of Ni, Co, Zn, Cu, Ba, Th and Na_2O which reflects a hydrothermal activity. The Pb, As and Sr are correlated to Ca and Mn and that is in greater part the result of diagenetic migration.

Medvednica Mt. The trace elements on the diagram are separated into three different groups (Fig. 4). The first, terrigenous group is correlated to Al_2O_3, TiO_2, K_2O, Na_2O and MgO, while the second hydrothermal group correlates to Fe, P and Mn (probably adsorbed on Fe-Mn hydroxide precipitates). The third group consists of V, Co, Y and As, and indicates an enrichment of these elements during the diagenesis.

Žumberak Mt. The diagram (Fig. 4) shows two different groups of trace elements. In contrast to the previously discussed areas with predominant terrigenous major elements (Al_2O_3, TiO_2 and K_2O), the trace elements Cu, Sr and Y are strongly correlated to iron and phosphorus indicating a possibly weaker hydrothermal activity (together with Ni, Cr, Ba, As and Na_2O) and increased terrigenous input of these elements along with Zr, Hf, Th, Cr and others. The second separated group consists of Zn, Pb, Ca, Mg and Mn. The grouping of these elements is more the result of migration during diagenetic and postdiagenetic processes (silicification, dolomitization) than of direct magmatic activity.

We normalized the major and trace elements to Al, and placed them into relationship to NASC ("North American shale composite"; Gromet et al. 1984) (Fig. 5). This diagram shows the enrichment of SiO_2 in all samples, which confirms the aforementioned diagenetic migration. K, Ti and Rb concentration have quite similar normalized values according to the NASC. Mg, Fe and Na also belong to the same group. Fe on the Ivanščica Mt is enriched and reflects a hydrothermal input into the sediment (high Fe content; Table 1). Ca is depleted

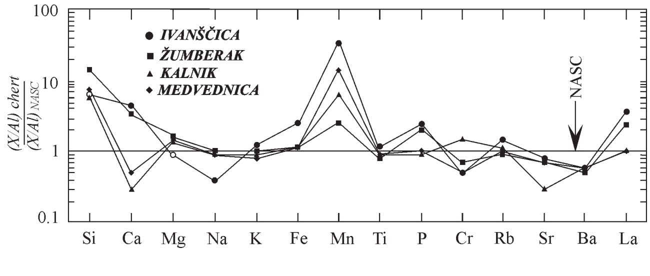

Fig. 5. Al-normalized major and trace elements distribution relative to NASC (NASC values from Gromet et al. 1984; detailed description see text).

on the Kalnik and Medvednica Mts, which indicates sedimentation without a carbonate component (probably below the CCD). Increased ratios of Ca on Ivanščica and Žumberak Mts reflect the influence of carbonate host sediment. However, a portion of CaO is of secondary origin because of the underlying carbonate sediments (limestones and dolomites) which partly migrated in cherts during diagenesis. Manganese enrichment in relation to NASC is probably ambiguous. This enrichment starts with a hydrothermal input of Mn, and it continues with a remobilization and reprecipitation in more oxidic, or as carbonate in reducing conditions. Phosphorus on the Kalnik and Medvednica Mts is quite similar to NASC contents and is here probably of terrigenous origin (apatite as a heavy mineral), while the increased contents on the Ivanščica and Žumberak Mts indicate an additional source (adsorption on Fe and Mn hydroxide).

REE

The content of the majority of REE in the analysed radiolarian cherts is relatively low (<1mg/kg) (Table 3).

While analysing the correlation ratios of ΣREE to major elements (Fig. 6) it can be concluded that the REE on the Kalnik, Medvednica and Žumberak Mts are positively correlated to Al, Ti, K and Na, which means that the aluminosilicates are significant carriers of REE in radiolarian cherts. Additionally, the high correlation coefficient of ΣREE to Zr and Ti indicates that the heavy minerals from the terrigenous component are partly carriers of rare earths. REE in the analysed cherts show no correlation to Mn (besides a weaker correlation on Kalnik Mt; r = 0.71, not shown), which is the result of diagenetic fractionation of Mn and its migration from silica rich layers. On the other hand, there is a significant connection of ΣREE to Fe on the Ivanščica Mt (Fig. 6), while it is weaker to P and Fe in the other three areas. This indicates that a part of REE was adsorbed onto Fe-hydroxide from sea water during sedimentation (in sample BD-II/4 on the Ivanščica Mt ΣREE is 213.99 mg/kg with a 17.27 % of iron) and probably onto Mn (the Mn content in the sample BD-16 is >1 %).

We normalized our REE data to NASC (normalization values from Gromet et al. 1984). These average shale values are the best representatives of the upper continental crust REE values and of the REE distribution of average values for terrestrial material in the oceans (Condie 1991).

REE distribution patterns for the Kalnik and Medvednica radiolarian cherts are relatively flat, but show slight LREE enrichment compared to HREE (Fig. 7) (average of ratio La_n/Yb_n 1.24 and 1.29 respectively; Table 3). The radiolarian cherts on the Ivanščica and Žumberak Mts show a stronger enrichment of LREE compared to HREE (average of ratio La_n/Yb_n 1.41 and 1.80 respectively; Table 3). There is a difference in REE content between the studied sections on Žumberak Mt, but their basic characteristics are quite similar (Fig. 7). The LREE values on the Kalnik and Medvednica Mts are quite similar to

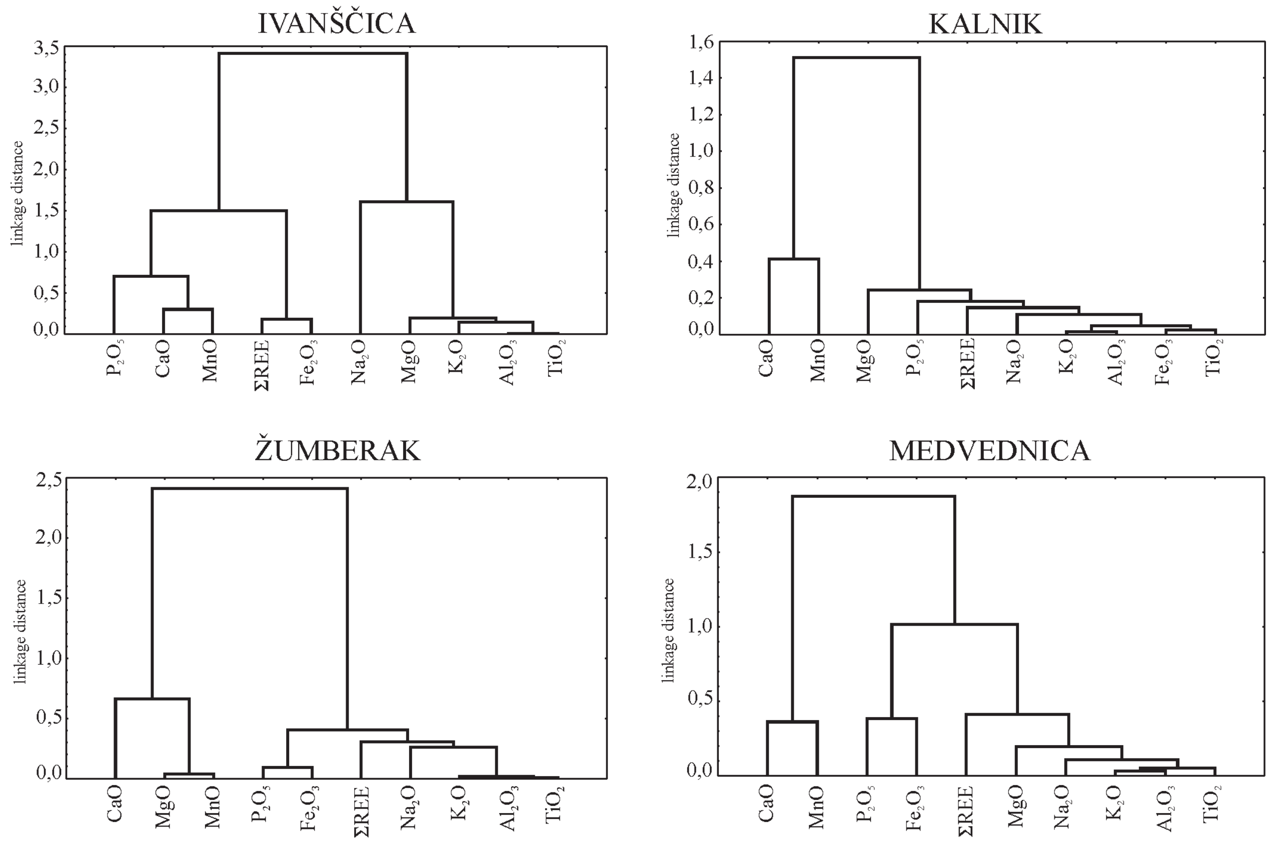

Fig. 6. Cluster analysis diagrams of major elements and ΣREE (Tree clustering; Linkage rule = Ward's method; Distance measure = 1-Pearson r).

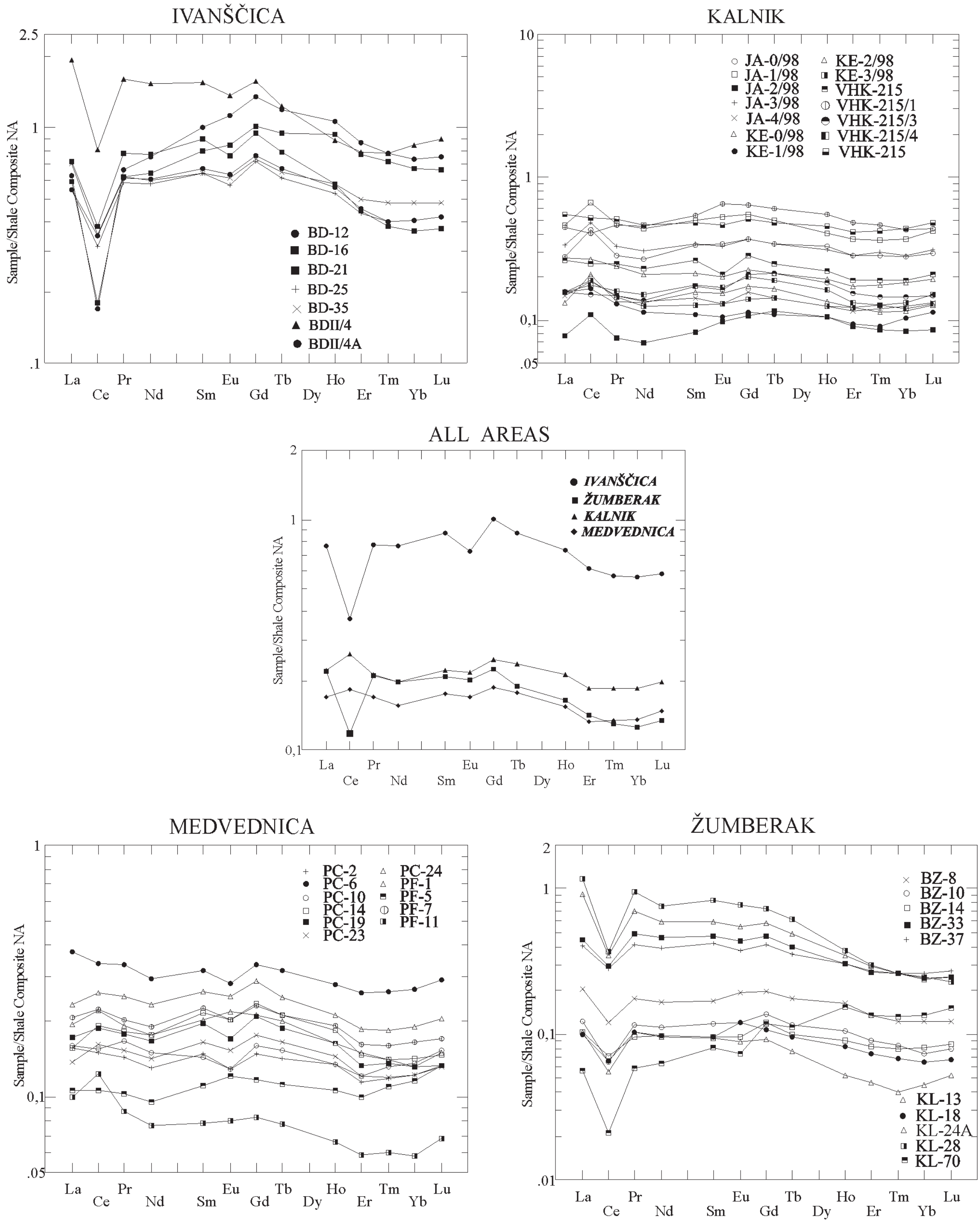

Fig. 7. NASC normalized REE distribution diagrams for all samples. The values on the diagram in the middle are geometric means values for individual areas.

the proposed values of La_n/Yb_n for the marine sediments (Sholkovitz 1990; $La_n/Yb_n = 1.33+/-0.15$), but they are higher on Ivanščica and Žumberak Mts.

It is significant for Ivanščica and Žumberak radiolarian cherts that they have a distinctive negative Ce anomaly (Ce/Ce*) (mean for Ce/Ce* 0.46 and 0.58; Table 3), while this anomaly is positive on Kalnik and Medvednica Mts (mean for Ce/Ce* 1.17 and 1.31). It is well known that the Ce/Ce* does not change during diagenetic processes in most cases, so the difference of registered values presents a variation in the primary sediment (Murray et al. 1992a). The marked negative Ce anomalies are characteristic of deep sea sediments (Shimizu & Masuda 1977; Toyoda et al. 1990; Murray et al. 1990, 1991).

The positive Ce anomaly could be caused by an increased terrigenous input (Murray et al. 1992a). We could give two explanations for the positive Ce anomaly on Kalnik and Medvednica Mts (1) the deposited radiolarian oozes originally had a negative Ce anomaly. During the diagenetic processes the partial depletion of LREE occurred except for Ce, which was followed by the development of a positive Ce anomaly (Murray et al. 1991) and (2) the positive Ce anomaly could be the result of an “oxygen minimum zone” (OMZ), which develops close to a continent in narrow basins as a result of a high primary plankton production in connection with increased oxygen consumption for oxidation of organic matter (Murray et al. 1990). It should be mentioned that almost all analysed samples from Kalnik and Medvednica Mts are red in colour and were probably deposited below the OMZ. A direct influence of the OMZ to the positive Ce anomaly in these rocks thus cannot be confirmed.

Depositional environments

Bedded cherts (radiolarites *s.str.*) originate in specific geotectonic conditions and are connected to specific evolution phases of ocean basins and continental margins. In most cases they are the only sediments in the ophiolite sequence with a valid fossil content. Besides that, the chert sequences can today often be found in structurally alochthonous packages, whereby they represent carriers of important information about the evolution of the sedimentary basin, and play an important role as a stratigraphic and depositional indicator for the paleogeographical reconstruction of particular areas or regions.

In the past decade, the use of chemical methods has gained significance, and today these methods represent an important tool for solving the problems of depositional environments of radiolarian cherts, and simultaneously for determination of the paleogeographical position of sedimentary basins during their genesis.

Because of the diagenetic chemical fractionation and the migration of Si, Mn, Ca, Mg, P, Sr and Ba out of silica rich layers, these elements are inappropriate for the determination of depositional environment. Therefore we used only the diagrams based on Al, Fe, La and Ce proposed by Murray (1994).

On the La_n/Ce_n vs. $Al_2O_3/(Al_2O_3+Fe_2O_3)$ diagram (La and Ce NASC normalized) (Fig. 8), the Kalnik and Medvednica samples are grouped in the continental margin field. A smaller part of Žumberak radiolarian cherts belong to the pelagic field,

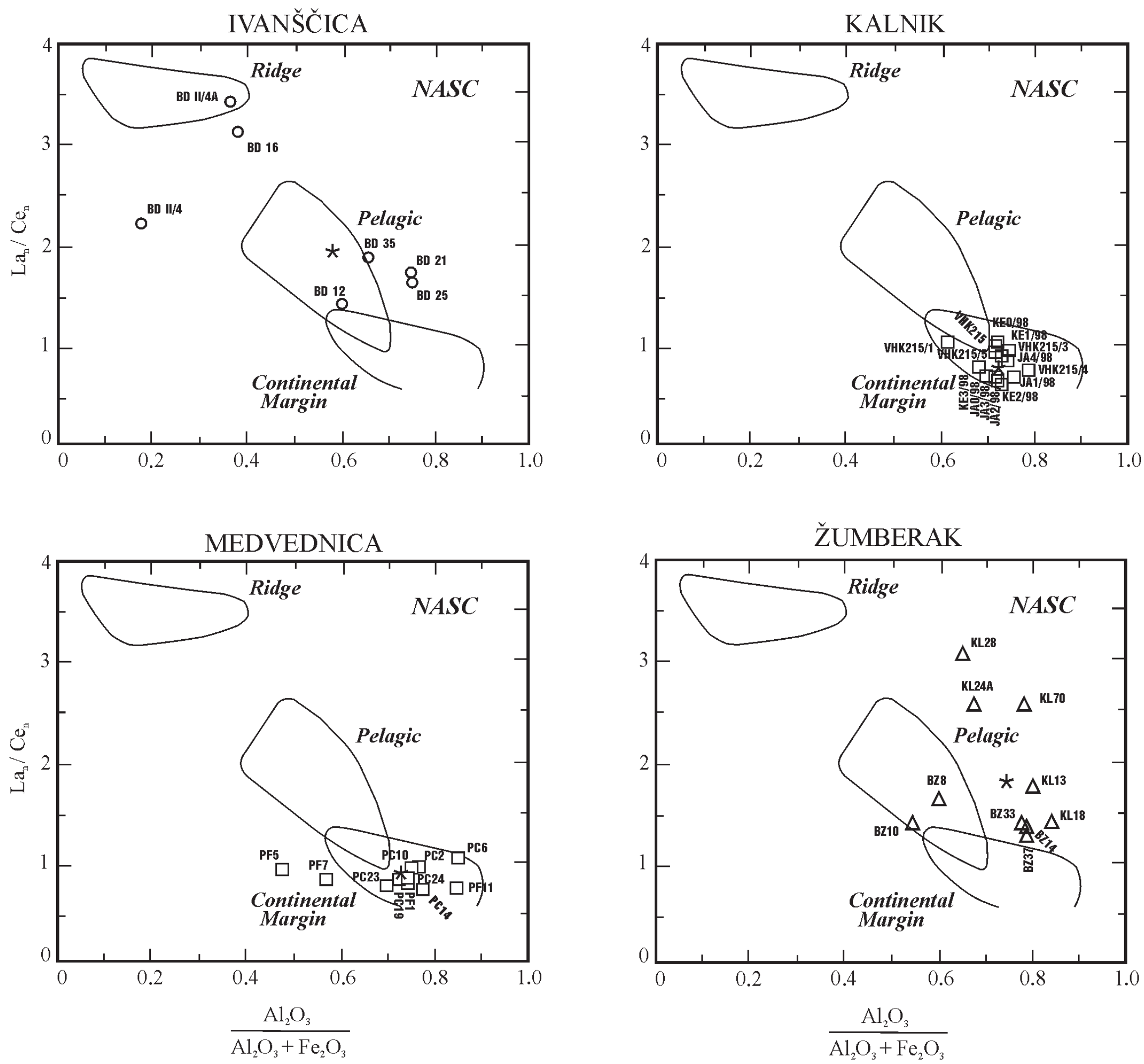

Fig. 8. La_n/Ce_n vs. Al_2O_3/ $Al_2O_3+Fe_2O_3$ discrimination diagrams for individual investigated areas (individual fields after Murray 1994).

but the majority is outside of all fields. Such a distribution is conditioned by the increase of the La_n/Ce_n ratio and by a lower content of Ce in those samples. The samples on Ivanščica Mt are divided into two groups. One group is closer to the pelagic field, with a lower $Al_2O_3/(Al_2O_3+ Fe_2O_3)$ ratio due to increase of Fe content, and a decrease of Ce content. Three samples are grouped closely to the field of the mid-oceanic ridge. The distribution of these samples is the result of a further increase of Fe content, and the decrease of Ce content (Table 3), which caused an increase of the La/Ce ratio.

The sample distribution on the diagrams is not completely in concordance with the geological data. In fact, the radiolarian cherts on Kalnik Mt lie between basic effusive rocks or directly on them, and in the diagrams they belong to the continental margin field. This is a result of the width of the sedimentary basin (increased terrigenous input in a narrow sedimentary trough). The radiolarian chert samples on Ivanščica Mt lie on carbonate sediments (Fig. 2), while a part of the samples on the discussed diagrams show a strong influence of the ocean ridge (Fig. 8). Lower terrigenous input is a consequence of the sedimentary basin's size, as the disintegrating carbonate platform created a larger distance to the continent.

Based on geological data from previous studies (Halamić & Goričan 1995; Bukovac et al. 1995; Halamić 1998; Grgasović et al. 2000) and geochemical data in this paper, we constructed a simplified evolutionary model of the sedimentary basin during the Triassic in which the studied radiolarian cherts were sedimented (Fig. 9).

The disintegration of the carbonate platform in the studied areas started probably in Middle Anisian (rifting), which is documented by a sudden facies change (sections on the Žumberak and Ivanščica Mts). The subsequent disintegration and deepening of the sedimentary basin during the Late Anisian and Early Ladinian was accompained by magmatic activity (MOR-basalts on Medvednica Mt; Halamić et al. 1998 and the VHK section on Kalnik Mt). The magmatic activity on Žumberak and Ivanščica Mts is registered only in the form of tuffs and tuffites. During the following spreading and lateral drift of the sedimentary basin the Žumberak and Ivanščica areas stayed at the basin's margin (passive continental margin),

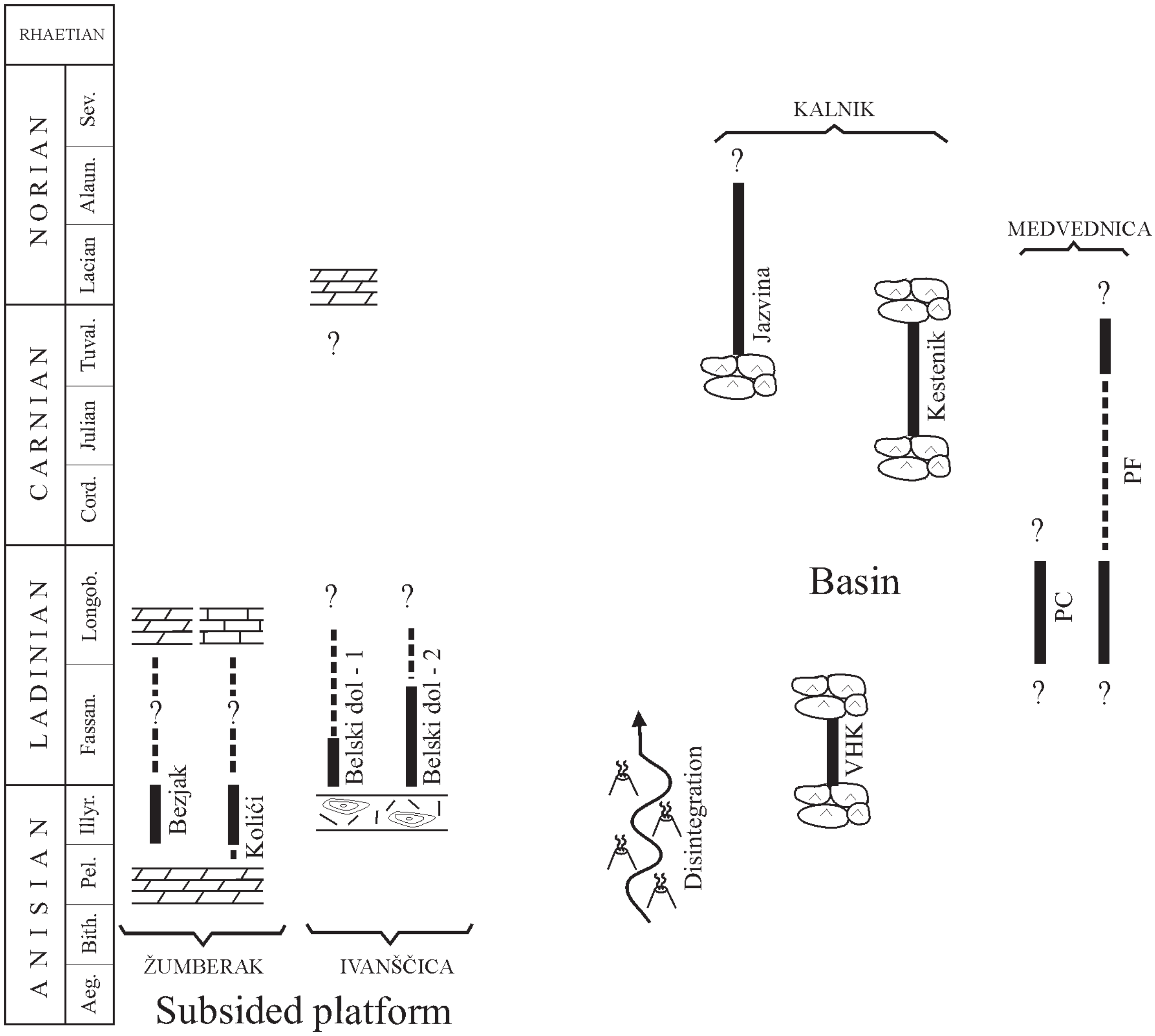

Fig. 9. Simplified disintegration model of the carbonate platform and position of investigated radiolarian cherts during the Triassic (legend see Fig. 2).

while the Medvednica and Kalnik Mts were located in the deeper part of the same basin. The most distinctive differentiation between the Žumberak and Ivanščica Mts on the one side and the Medvednica and Kalnik Mts on the other, happened from Late Ladinian (Late Carnian?) when the carbonate sedimentation on Žumberak and Ivanščica Mts was renewed. At the same time on the Medvednica and Kalnik Mts the magmatic activity and sedimentation of radiolarian siliceous mud continued.

Conclusions

All of the analysed radiolarian cherts are rocks with high SiO_2 content (mean SiO_2 = 90.05 %). The major part of SiO_2 is of biogenic origin (radiolarian tests). The SiO_2 enrichment of particular layers in the radiolarite and the shale/chert alternation is the result of diagenetic chemical fractionation of SiO_2 and its migration (Murray et al. 1992c; Murray 1994). Statistical analysis (correlation) and the normalization to Al compared to NASC of major and trace elements showed that besides the siliceous component, two other components stand out in the radiolarian cherts. One of them is detritic (terrigenous input) and it consists of Al, Ti, K, Cr, Hf, Zr, Th, Rb, Sc and Nb. All these elements show a relatively high mutual correlation (Fig. 3 and 4). The other component (hydrothermal) consists of iron, manganese and phosphorus, which precipitated into the precursor sediment on the divergent plate margins, in the form of hydroxides with a high adsorption capability. Phosphate is adsorbed onto Fe-hydroxide. Subsequently, during diagenesis goethite was formed from Fe-hydroxide and apatite from phosphate. In this process, manganese is more sensitive to redox conditions than iron, and is therefore dissolved, removed and reprecipitated and now shows no significant correlation to Fe and P.

The La/Ce vs. Al/Al+Fe ratios (Fig. 8) suggest that (1) the radiolarian cherts from the Kalnik and Medvednica Mts were sedimented near a continental margin (narrow sedimentary trough). That is also indicated by a positive Ce anomaly which ranges from 1.17 to 1.31 (Table 3) and these values are characteritic for sedimentary basins lying closer to the continental masses (Murray et al. 1990), (2) the Ivanščica radiolarian cherts were deposited in a pelagic environment with mid-ocean ridge influence and (3) the siliceous rocks from Žumberak Mt were sedimented in an open sea environment without mid-ocean influence.

The distinctive negative Ce-anomalies on Ivanščica and Žumberak Mts indicate a reduced terrigenous input, or an open sea sedimentary environment (Ce/Ce* from 0.46 to 0.58). Since the cherts on those two terrains are sedimented directly onto the dolomites and limestones of the carbonate platform (Bukovac et al. 1995), the radiolarian cherts were not necessary sedimented in a deep water environment (a negative Ce anomaly was also registered in Triassic carbonate sedimented on a 50 m depth; Liu et al. 1988). The terrigenous input in this part of the sedimentary basin was probably weaker, because of the width of the disintegrated carbonate platform (greater distance from the continent) or because of a topographically higher position (bypass of fine terrigenous material) with respect to Medvednica and Kalnik.

Acknowledgment: The authors are grateful to Dr. J. Michalík (Bratislava), Dr. S. Kovács (Budapest), Prof. I. Rojkovič (Bratislava) and two anonymous reviewers for critical comments that have improved this manuscript. The work was done in the framework of the geological mapping of Croatia (scale 1:50,000) with support of the Croatian Institute of Geology and Croatian Ministry of Science and Technology, Project 01810106.

References

Aitchison J. 1986: The statistical analysis of compositional data. *Chapman and Hall*, 1–416.

Basch O. 1983: Explanatory notes for sheet Ivanić Grad. *Inst. za geol. istraž.* Zagreb, *Savezni geol. zavod* Beograd, 66 (in Croatian with English summary).

Berner R.A. 1973: Phosphate removal from seawater by adsorption on volcanic ferric oxides. *Earth Planet. Sci. Lett.* 18, 77–86.

Bukovac J., Grgasović T., Glovacki-Jernej Ž., Jerinić G., Galović I. & Prtoljan B. 1995: Lithostratigraphic division of Triassic dolomite deposits in SW Žumberak Mt. under the works on the geological map of the Republic of Craotia 1:50,000. In: Vlahović I., Velić I. & Šparica M. (Eds.): *1. Croatian Geological Congress. Proceedings*, Zagreb, 1, 137–142 (in Croatian with English abstract).

Condie K.C. 1991: Another look at rare earth elements in shales. *Geochim. Cosmochim. Acta* 55, 2527–2531.

Grgasović T., Halamić J., Goričan Š., Slovenec Da. & Kolar-Jurkovšek T. 2000: Triassic deep water sediments of selected localities in northwestern Croatia: In: Vlahović I. & Biondić R. (Eds.): *2. Croatian Geological Congress. Proceedings*, Zagreb, 181–189 (in Croatian with English abstract).

Gromet L.P., Dymek R.F., Haskin L.A. & Korotev R.L. 1984: The "North American shale composite": Its compilation, major and trace element characteristics. *Geochim. Cosmochim. Acta* 48, 2469–2482.

Gundlach H. & Marchig V. 1982: Ocean floor "metalliferous sediments" — two possibilities for genesis. In: Amstutz G.C., El Goresy A., Frenzel G., Kluth C., Moh G., Wauschkuhn A. & Zimmermann R.A. (Eds.): Ore genesis — the state of the art. *Springer Verlag*, Berlin Heidelberg, 200–210.

Haas J., Császár G., Kovács S. & Vörös A. 1990: Evolution of the Western Part of the Tethys as reflected by the geological formations of Hungary. *Acta Geod. Geoph. Mont. Hung.* 25, 3–4, 325–344.

Haas J., Kovács S., Krystyn L. & Lein R. 1995: Significance of Late Permian-Triassic facies zones in terrane reconstructions in the Alpine-North Pannonian domain. *Tectonophysics* 242, 19–40.

Haas J., Mioč P., Pamić J., Tomljenović B., Árkai P., Bérczi-Makk A., Koroknai B., Kovács S. & Felgenhauer E.-R. 2000: Complex structural pattern of the Alpine-Dinaridic-Pannonian triple junction. *Int. J. Earth Sci.* 89, 2, 377–389.

Halamić J. 1998: The lithostratigraphic characterisation of Jurassic and Cretaceous sediments with ophiolite of Mts. Medvednica, Kalnik and Ivanščica. *Unpubl. Phil. Thesis, University of Zagreb, Faculty of Natural and Mathematics Sciences*, Zagreb, 1–180 (in Croatian with English summary).

Halamić J., Slovenec Da. & Kolar-Jurkovšek T. 1998: Triassic pelagic limestones in pillow lavas in the Orešje Quarry near Gornja Bistra, Medvednica Mt. (Northwest Croatia). *Geol. Croatica* 51, 1, 33–47.

Halamić J. & Goričan Š. 1995: Triassic Radiolarites from Mts. Kalnik and Medvednica (Northwestern Croatia). *Geol. Croatica* 48, 2, 129–146.

Herak M. 1986: A new concept of geotectonics of the Dinarides. *Acta Geol. (Zagreb)* 16, 1, 1–42.

Herak M., Jamičić D., Šimunić A. & Bukovac J. 1990: The northern boundary of the Dinarides. *Acta Geol. (Zagreb)* 20, 1, 5–27.

Klosa D. 1994: Eine rechnergestützte Methode zur Bestimmung des Gesamtkarbonatgehaltes in Sedimenten und Böden. *Z. Angew. Geol.* 40, 18–21.

Kovács S., Császár G., Galácz A., Haas J., Nagy E. & Vörös A. 1988: The Tisza Superunit was originally part of the North Tethyan (European) margin. In: Rakús M., Dercourt J. & Nairn A.E.M. (Eds.): Evolution of the Northern margin of Tethys: The results of IGCP Project 198. *Mém. Soc. Géol. France*, 2, 81–100.

Liu Y.-G., Miah M.R.U. & Schmitt R.A. 1988: Cerium: A chemical tracer for paleo-oceanic redox conditions. *Geochim. Cosmochim. Acta* 52, 1361–1371.

Marchig V., Gundlach H., Möller P. & Schley F. 1982: Some geochemical indicators for discrimination between diagenetic and hydrothermal metalliferous sediments. *Marine Geol.* 50, 241–256.

Marchig V., Erzinger J. & Heinze P-M. 1986: Sediment in the black smoker area of the East Pacific Rise (18,5°S). *Earth Planet. Sci. Lett.* 79, 93–106.

Marchig V., Erzinger J. & Rösch H. 1987: Sediments from a hydrothermal field in the central valley of the Galapagos rift spreading center. *Marine Geol.* 76, 243–251.

Murray R.W. 1994: Chemical criteria to identify the depositional environment of chert: general principles and applications. *Sedimentary Geol.* 90, 213–232.

Murray R.W., Buchholtz ten Brink M.R., Jones D.L., Gerlach D.C. & Russ III G.P. 1990: Rare earth elements as indicators of different marine depositional environments in chert and shale. *Geology* 18, 268–271.

Murray R.W., Buchholtz ten Brink M.R., Brumsack H.J., Gerlach D.C. & Russ III G.P. 1991: Rare earth elements in Japan Sea sediments and diagenetic behavior of Ce/Ce*: Results from ODP Leg 127. *Geochim. Cosmochim. Acta* 55, 2453–2466.

Murray R.W., Buchholtz ten Brink M.R., Gerlach D.C., Russ III G.P. & Jones D.L. 1992a: Rare earth, major, and trace element composition of Monterey and DSDP chert and associated host sediment: Assessing the influence of chemical fractionation during diagenesis. *Geochim. Cosmoschim. Acta* 56, 2657–2671.

Murray R.W., Buchholtz ten Brink M.R., Gerlach D.C., Russ III G.P. & Jones D.L. 1992b: Interoceanic variation in the rare earth, major, and trace element depositional chemistry of chert: perspectives gained from the DSDP and ODP record. *Geochim. Cosmochim. Acta* 56, 1897–1913.

Murray R.W., Jones D.L. & Buchholtz ten Brink M.R. 1992c: Diagenetic formation of bedded chert: Evidence from chemistry of the chert–shale couplet. *Geology* 20, 271–274.

Pamić J. & Tomljenović B. 1998: Basic geological data on the Croatian part of the Zagorje-Mid-Transdanubian Zone. *Acta Geol. Hungarica* 41, 389–400.

Rangin C., Steinberg M. & Bonnot-Courtois C. 1981: Geochemistry of the Mesozoic bedded chert of Central Baja California (Vizcaino-Cedros-San Benito): implications for paleogeographic reconstruction of an old oceanic basin. *Earth Planet. Sci. Lett.* 54, 313–322.

Ruitz-Ortiz P.A., Bustillo M.A. & Molina J.M. 1989: Radiolarite sequences of the Subbetic, Betic Cordillera, Southern Spain. In: Hein J.R. & Obradović J. (Eds.): Siliceous deposits of the Tethys and Pacific regions. *Springer Verlag,* 107–127.

Shimizu H. & Masuda A. 1977: Cerium in chert as an indication of marine environment of its formation. *Nature* 266, 346–348.

Sholkovitz E.R. 1990: Rare-earth elements in marine sediments and geochemical standards. *Chem. Geol.* 88, 333–347.

Swan A.R.H. & Sandilands M. 1996: Introduction to geological data analysis. *Blackwell Science,* Oxford, 1–446.

Šikić K., Basch O. & Šimunić A. 1979: Explanatory notes for sheet Zagreb. *Inst. za geol. istraž.* Zagreb, *Savezni geol. zavod* Beograd, 66 (in Croatian with English summary).

Šimunić An., Pikija M., Hećimović I. & Šimunić Al. 1981: Explanatory notes for sheet Varaždin. *Inst. za geol. istraž.* Zagreb, *Savezni geol. zavod* Beograd, 66 (in Croatian with English summary).

Šimunić Al. & Šimunić An. 1980: Petrographic composition and genesis of Triassic deposits of Ivanščica, Kalnik and Ravna Gora Mountain. *Geološki Vjesnik (Zagreb)* 32 (1979), 243–253 (in Croatian with English summary).

Šimunić An. & Šimunić Al. 1997: Triassic deposits of Hrvatsko Zagorje. *Geol. Croatica* 50, 2, 243–250.

Toyoda K., Nakamura Y. & Masuda A. 1990: Rare earth elements of Pacific pelagic sediments. *Geochim. Cosmochim. Acta* 54, 1093–1103.

Wilson M. 1989: Igneous petrogenesis — A global tectonic approach. *Unwin Hyman,* London, 1–465.